Z. Physik C, Particles and Fields 4, 237–256 (1980)

Zeitschrift für Physik C Particles and Fields

Two- and Three-point Energy Correlations in Hadronic e^+e^- Annihilation*

Geoffrey C. Fox and Stephen Wolfram**
California Institute of Technology, Pasadena, CA91125, USA

Abstract. Correlations between the energies incident on two or three detectors around e^+e^- annihilation events are considered as a probe of the QCD structure of the events. Practical methods for deducing two-detector energy correlations (which give the mean product of energies incident on two detectors as a function of their angular separation) from measured events are devised. Analytical formulae for energy correlations from QCD perturbation theory are given, but it is found that large corrections from hadron formation obscure these asymptotic predictions at available energies. Correlations between the final state and the incoming $e^\pm$ beam direction are discussed, and observables are presented which measure the angular distributions of planes of final particles with respect to the beam axis (but do not require explicit determination of the planes). Finally, three-detector energy correlations and their moments are treated, and methods for investigating planar structures in e^+e^- annihilation events are devised.

1. Introduction

In a previous paper [1][1], we introduced the shape parapeters (the P_l are the Legendre polynomials, and the sum runs over all pairs of particles)

$$H_l = \sum_{i,j} \frac{|\mathbf{p}_i|\,|\mathbf{p}_j|}{s} P_l(\hat{p}_i \cdot \hat{p}_j) \tag{1.1}$$

which describe the distribution of energy in the final states of e^+e^- annihilation events and whose mean values may be computed from QCD perturbation theory. In this paper, we describe further methods for analyzing event shapes[2]. In Sect. 2, we consider two-point energy correlations, whose mean values provide a reexpression of the information on event shapes contained in the $\langle H_l \rangle$. The H_l were explicitly constructed to be rotationally invariant; Sect. 3 discusses a generalization of the H_l in which measures correlations between the final state and the incoming beam direction.

We define the two-detector energy correlation function introduced in [1] and [3] by

$$\tilde{F}_2(\sigma_1, \sigma_2) = \frac{16\pi^2}{|\sigma_1|\,|\sigma_2|} \frac{|\mathbf{p}_1|\,|\mathbf{p}_2|}{s}, \tag{1.2}$$

where the $|\mathbf{p}_i|$ are the sum of the moduli of the three-momenta of particles incident on two detectors covering the regions σ_i of total solid angle $|\sigma_i|$. The rotationally-invariant observable F_2 is formed in each event by averaging $\tilde{F}_2$ over all possible positions for the detectors, while maintaining their relative orientation. F_2 may, therefore, be written as

$$F_2(\chi) = \frac{\langle |\mathbf{p}_1|\,|\mathbf{p}_2| \rangle_0}{\langle E_1 \rangle_0 \langle E_2 \rangle_0} \simeq \frac{\langle E_1 E_2 \rangle_0}{\langle E_1 \rangle_0 \langle E_2 \rangle_0}, \tag{1.3}$$

where χ signifies the relative orientation of σ_1 and σ_2, and the averages are over all positions of σ_1 and σ_2 in a particular event which maintain this: F_2 does not depend on the orientation of the final state with respect to the beam axis. For theoretical purposes, such as those of [2] and [4], it is convenient to consider the idealized energy correlation $F_2^{pt}(\chi)$ between two point

* Work supported in part by the U.S. Department of Energy under Contract No. DE-AC-03-79ER0068
** Supported by a Feynman fellowship

1 The background and motivation of the present work is discussed in [1]. As in [1], $e^+e^- \to q\bar{q}(GG\ldots)$ represents the sum of processes $e^+e^- \to q\bar{q}$, $e^+e^- \to q\bar{q}G$, $e^+e^- \to q\bar{q}GG$ and so on, together with virtual (loop) corrections to these. ζ denotes a ${}^3S_1$ $Q\bar{Q}$ heavy quark bound state (such as ψ or Υ). Another notation from [1] is the kinematic definition $x_i = 2E_i/\sqrt{s}$

2 The material in this paper consists mainly of Sects. 4–6 of the preprint [2]

0170-9739/80/0004/0237/$04.00

detectors. This has the useful property that

$$H_l = \frac{1}{2}\int_{-1}^{1} F_2^{pt}(\chi) P_l(\chi) d\chi . \tag{1.4}$$

For large l, $P_l(\chi)$ may be approximated by

$$\begin{aligned} P_l(\cos\theta) &= 1 && |\theta| < 2/l \\ &= (-1)^l && |\pi - \theta| < 2/l \\ &= 0 && \text{otherwise}. \end{aligned} \tag{1.5}$$

Hence to obtain estimates for the $\langle H_l \rangle$ at large l, one requires only the behavior of $\langle F_2^{pt}(\chi)\rangle$ for χ close to ± 1, corresponding to energy correlations between detectors which are either close together or back-to-back (anticollinear). Such estimates are given in [2, 4, 5].

In order to assess to what extent the various predictions presented in this paper constitute tests of QCD, one should compare them with results from other theories. Appendix B gives some predictions which would follow from a theory with colored scalar, rather than vector, gluons.

2. Rotationally-Averaged Two-Detector Energy Correlations

2.1. Formalism and Calculational Techniques

In this section we discuss the rotationally invariant observable F_2 defined in (1.2). The two detectors used in this definition occupy areas $\sigma_i (i = 1, 2)$ which are, in general, of arbitrary shape. However for simplicity, we shall restrict ourselves in this paper to the case in which the σ_i are congruent circular patches of angular radius $\cos^{-1}(\delta)$. Hence $|\sigma_i| = 2\pi(1-\delta)$ and F_2 is a function only of χ and δ, where $\cos^{-1}(\chi)$ is the angle between the centers of the two detectors σ_i. The arrangement is illustrated in Fig. 1. The generalization of our treatment to detectors of arbitrary shape is

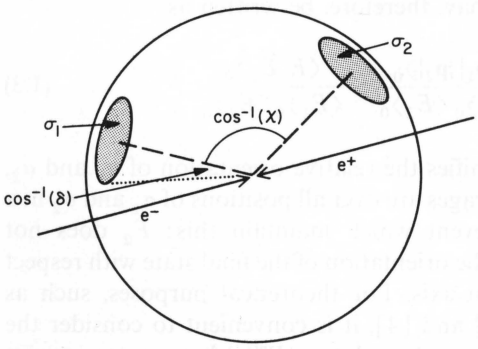

Fig. 1. Two circular detectors σ_1, σ_2 of half angle $\cos^{-1}(\delta)$. $\cos^{-1}(\chi)$ is angle between the centers of the detectors. $F_2(\chi, \delta)$ is obtained by averaging over all positions for the detectors which preserve the angle χ

straightforward. The best method of calculating F_2 from events appears to be the use of the formula

$$F_2(\chi;\delta) = 2\sum_{i,j} \frac{|\mathbf{p}_i|\,|\mathbf{p}_j|}{s} U(\chi;\delta;\cos\phi_{ij}), \tag{2.1}$$

where the sums on i and j run over all the particles in the event (including the case $i=j$). The smearing function U is given by

$$U(\chi;\delta;\cos\phi_{ij}) = \frac{1}{|\sigma_1|\,|\sigma_2|}\int d\hat{\Omega}_{d1}\, \Theta(\hat{n}_{d1}, \hat{n}_{pi}; \hat{n}_{d2}, \hat{n}_{pj}; \delta). \tag{2.2}$$

Here $\hat{n}_{dk}$ is a unit vector in the direction of detector k and $\hat{n}_{pi}$ the unit vector in the direction of particle i. If $\hat{\Omega}_{d1}$ runs over all elements of the rotation group, so that $\int d\hat{\Omega}_{d1} = 8\pi^2$, then

$$\begin{aligned} \hat{n}_{d1} &= \hat{\Omega}_{d1}\hat{z} \\ \hat{n}_{d2} &= \hat{\Omega}_{d1}\hat{R}(\chi)\hat{z}, \end{aligned} \tag{2.3}$$

where $\hat{z}$ is a unit vector in the z direction and $\hat{R}(\chi)$ a rotation through $\cos^{-1}(\chi)$ about the y axis. Finally in (2.2), the function Θ takes on the values 1 or 0, and is zero unless both the pairs $\hat{n}_{d1}, \hat{n}_{pi}$ and $\hat{n}_{d2}, \hat{n}_{pj}$ lie within an angle $\cos^{-1}(\delta)$ of each other, so that particle i is incident on detector 1 and particle j on detector 2. The rotational invariance of F_2 is exhibited by the fact that it has the same value for any choice of particle directions $\hat{n}_{pi}, \hat{n}_{pj}$ so long as the angle ϕ_{ij} between them remains fixed. For some purposes, it is more convenient to write U in the symmetrical form

$$\begin{aligned} U(\chi;\delta;\cos\phi_{ij}) = \frac{1}{8\pi^2|\sigma_1|\,|\sigma_2|}\int d\hat{\Omega}_{d1}\, d\hat{\Omega}_{pi} \\ \Theta(\hat{\Omega}_{d1}\hat{z}, \hat{\Omega}_{pi}z; \hat{\Omega}_{d1}R(\chi)\hat{z}, \hat{\Omega}_{pi}\hat{R}(\cos\phi_{ij})\hat{z}; \delta). \end{aligned} \tag{2.4}$$

Note that

$$\int_{-1}^{+1} U(\chi;\delta;\cos\phi_{ij})\, d\chi = 2 \tag{2.5}$$

which implies the same normalization for F_2:

$$\int_{-1}^{+1} F_2(\chi;\delta)\, d\chi = 2, \tag{2.6}$$

independent of the value of δ.

In the limit $\delta \to 1$, σ_1, and σ_2 become point detectors separated by an angle $\cos^{-1}(\chi)$. We define[3]

$$F_2^{pt}(\chi) \equiv \lim_{\delta\to 1}[F_2(\chi;\delta)]. \tag{2.7}$$

In this case, U becomes simply

$$U(\chi;1;\cos\phi_{ij}) = \delta(\chi - \cos\phi_{ij}), \tag{2.8}$$

3 In [1], $F_2^{pt}(\chi)$ was called simply $F(\chi)$

and we may rewrite[4]

$$F_2^{pt}(\chi)=2\sum_{i,j}\frac{|\mathbf{p}_i|\,|\mathbf{p}_j|}{s}\,\delta(\chi-\cos\phi_{ij}) \tag{2.9}$$

and

$$F_2(\chi;\delta)=\int_{-1}^{+1}d\chi'\,F_2^{pt}(\chi')\,U(\chi;\delta;\chi'). \tag{2.10}$$

F_2 may be expressed in terms of the H_l, defined in (1.1) as

$$H_l\equiv\left(\frac{4\pi}{2l+1}\right)\sum_{m=-l}^{+l}\left|\sum_i Y_l^m(\Omega_i)\frac{|\mathbf{p}_i|}{\sqrt{s}}\right|^2$$

$$=\sum_{i,j}\frac{|\mathbf{p}_i|\,|\mathbf{p}_j|}{s}\,P_l(\cos\phi_{ij}), \tag{2.11}$$

where the indices i and j run over the hadrons which are produced in the event, and ϕ_{ij} is the angle between particles i and j. When the first form for the H_l is used, a particular set of axis must be chosen to evaluate the angles (Ω_i) of the momenta, but the values of the H_l deduced will be independent of the choice. The Legendre expansion of F_2 is

$$F_2(\chi;\delta)=\sum_l(2l+1)H_l(\delta)P_l(\chi), \tag{2.12}$$

where the H_l as defined in (2.11) are $H_l(1)$, and correspondingly,

$$F_2^{pt}(\chi)=\sum_l(2l+1)H_lP_l(\chi). \tag{2.13}$$

The relation between $H_l(\delta)$ and H_l is

$$H_l(\delta)=\sum_{i,j}\frac{|\mathbf{p}_i|\,|\mathbf{p}_j|}{s}\int_{-1}^{+1}d\chi\,P_l(\chi)\,U(\chi;\delta;\cos\phi_{ij}) \tag{2.14}$$

so that (for circular detectors)

$$H_l(\delta)=\frac{I_l^2(\delta)}{(1-\delta)^2}H_l, \tag{2.15}$$

or equivalently

$$U(\chi;\delta;\cos\phi_{ij})=\sum_l\frac{(2l+1)I_l^2(\delta)P_l(\chi)P_l(\cos\phi_{ij})}{2(1-\delta)^2} \tag{2.16}$$

which clearly illustrates the symmetry between χ and $\cos\phi_{ij}$ also visible in (2.4). $I_l(x)$ was defined in [1] as

$$I_l(x)=\int_x^1 P_l(y)\,dy=\sqrt{1-x^2}\,P_l^{-1}(x). \tag{2.17}$$

4 In practical calculations, $F_2^{pt}(\chi)$ can be found easily from (2.9), and then (2.10) can be used to obtain $\langle F_2(\chi,\delta)\rangle$. Alternatively, one may use the rapidly convergent series (2.12). The latter method has the advantage that it also allows the calculation of the distribution $1/\sigma\,d\sigma/dF_2$. It is clear that for both means and distributions, the H_l are somewhat easier to extract from events than the energy correlation F_2

Note that as $l\to\infty$, $H_l\sim 1$ but $H_l(\delta<1)\sim 1/l^3$. Thus the series (2.12) is always absolutely convergent whereas (2.13) diverges (for point particles).

$F_2(\chi;\delta)$ receives a contribution from events in which the same particle passes through both detectors. Although this is of little practical interest, it must be kept if the normalization condition (2.6) is to be maintained. In the point detector limit, $\delta=1$, this configuration contributes to $F_2^{pt}(\chi)$ a term

$$F_2^{\text{same}}(\chi)=2\sum_i\frac{|\mathbf{p}_i|^2}{s}\,\delta(1-\chi), \tag{2.18}$$

where the coefficient of the delta function is related to the asymptotic limit of the H_l by

$$\frac{1}{2}\lim_{l\to\infty}[H_{2l}+H_{2l+1}]=\sum_i\frac{|\mathbf{p}_i|^2}{s}. \tag{2.19}$$

2.2. $e^+e^-\to q\bar{q}(G)$

In this section, we discuss mostly the idealized point detector energy correlation $F_2^{pt}(\chi)$: results for finite detectors may be obtained by the smearing (2.10).

All $e^+e^-\to q\bar{q}$ events give

$$F_2^{pt}(\chi)=[\delta(1-\chi)+\delta(1+\chi)]. \tag{2.20}$$

Three-particle final states give rise to a distribution of forms for $F_2^{pt}(\chi)$. Taking the fractional energies of the particles to be $x_i=\frac{2E_i}{\sqrt{s}}$, $\langle F_2^{pt}(\chi)\rangle$ becomes

$$\langle F_2^{pt}(\chi)\rangle=\sum_{\substack{i,j\\ i\neq j}}\frac{1}{2}\int_0^1 dx_i\,dx_j\,x_i\,x_j\frac{1}{\sigma}\frac{d\sigma}{dx_i\,dx_j}\cdot\left|\frac{\partial x_j}{\partial\cos\phi_{ij}}\right|\delta(x_j-\tilde{x}_j)+\frac{1}{2}\langle\sum x_i^2\rangle\,\delta(1-\chi), \tag{2.21}$$

where $\tilde{x}_j$ is determined by requiring that the angle ϕ_{ij} between particles i and j satisfies $\cos\phi_{ij}=\chi$, i.e.,

$$\tilde{x}_j=\frac{2(1-x_i)}{2+x_i(\chi-1)}. \tag{2.22}$$

The Jacobian is, therefore, simply

$$\left|\frac{\partial x_j}{\partial\cos\phi_{ij}}\right|=\frac{2x_i(1-x_i)}{[2+x_i(\chi-1)]^2}. \tag{2.23}$$

Hence the process $e^+e^-\to q\bar{q}(G)$ [which represents the sum of $e^+e^-\to q\bar{q}$ and $e^+e^-q\bar{q}G$ calculated to $0(\alpha_s)$]

gives[5]:

$$\langle F_2^{pt}(\chi)\rangle = \{\delta(1+\chi)+\delta(1-\chi)\} + \frac{16\alpha_s}{3\pi}\frac{(\chi+2)}{(1+\chi)(1-\chi)^5} \cdot \left\{4(\chi^2+4\chi+1)\log\left(\frac{1+\chi}{2}\right) + 3(1-\chi)(1+3\chi)\right\} + \{C_{-1}\delta(1+\chi)+C_{+1}\delta(1-\chi)\}, \tag{2.24}$$

and, for example

$$\langle F_2^{pt}(0)\rangle = \frac{32(3-4\log 2)\alpha_s}{3\pi} \simeq 0.77\alpha_s. \tag{2.25}$$

[The form of $\langle F_2(\chi;\delta=0.95)\rangle$ plotted in Fig. 2 is indistinguishable from (2.24) except very close to $\chi=\pm 1$ where the smeared delta function appear[6].]

The first term in (2.24) arises from the lowest-order process $e^+e^-\to q\bar{q}$. The second term accounts for the three-particle final state process $e^+e^-\to q\bar{q}G$. For $\chi\simeq -1$, this term becomes

$$-\frac{2\alpha_s}{3\pi}\left\{\frac{2\log\left(\frac{1+\chi}{2}\right)}{(1+\chi)} + \frac{3}{(1+\chi)} + \ldots\right\}, \tag{2.26}$$

while for $\chi\simeq +1$, the term is approximately

$$\frac{\alpha_s}{\pi}\left\{\frac{1}{(1-\chi)} + \frac{19}{30} + \ldots\right\}. \tag{2.27}$$

5 It is sometimes convenient to approximate $\langle F_2^{pt}(\chi)\rangle$ for $e^+e^-\to q\bar{q}G$ by the value obtained by performing the sum (2.21) only over the q and $\bar{q}$ and neglecting contributions from the gluon. In this case,

$$\langle F_2^{pt}(\chi)\rangle = \frac{8\alpha_s}{3\pi}\frac{1}{3(\chi-1)^5(1+\chi)}\left\{24(3\chi+5)\log\left(\frac{1+\chi}{2}\right) + (\chi-1)(\chi^2-14\chi-83)\right\}$$

so that

$$\langle F_2^{pt}(0)\rangle = \frac{8(120\log 2-83)\alpha_s}{9\pi} \simeq 0.05\alpha_s.$$

This is much smaller than the result (2.25) for the complete $q\bar{q}G$ final state since the q and $\bar{q}$ are rarely produced at 90°. Near $\chi=-1$, the $q\bar{q}$ contribution becomes

$$\frac{-2\alpha_s}{3\pi}\left\{\frac{2\log\left(\frac{1+\chi}{2}\right)}{(1+\chi)} + \frac{17}{3(1+\chi)} + \ldots\right\}:$$

the leading term here is the same as in (2.26) for the complete case, the subleading terms differ. For $\chi\simeq +1$, $\langle F_2^{pt}(\chi)\rangle$ calculated using only the q and $\bar{q}$ has no divergence and its regular part tends simply to $\alpha_s/30\pi$

6 In our phenomenological prescription for treating hadronic final states, we only consider $q\bar{q}G$ final states which have $H_2 < H_2^{cut}$. The form of $\langle F_2^{pt}(\chi)\rangle$ for $e^+e^-\to q\bar{q}G$ when $H_2^{cut}=0.8$ is qualitatively similar to the result (2.24) ($H_2^{cut}=1$), but there is a slight suppression near $\chi=\pm 1$

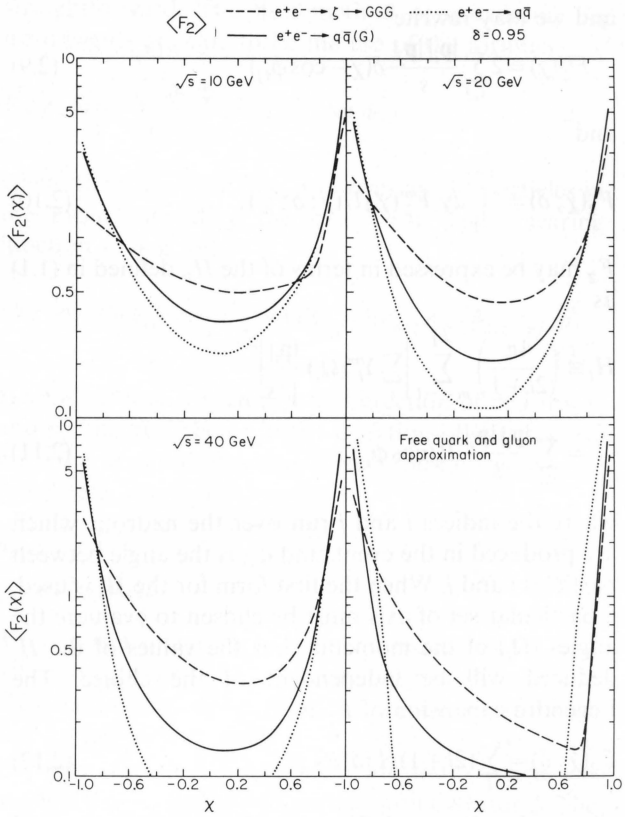

Fig. 2. The mean value of the rotationally invariant energy correlation F_2 as a function of detector separation χ for fixed detector size given by $\delta=0.95$ (opening angle $\simeq 18°$). The curves given are for simulated hadronic final states at $\sqrt{s}=10$, 20, and 40 GeV and in the approximation of free quarks and gluons. The free quark calculation marked $q\bar{q}(G)$ is, in fact, just the contribution of the $q\bar{q}G$ final state calculated with no H_2 cut and with no $q\bar{q}$ component added (this would contribute only at $\chi\simeq +1$)

The third term in (2.24) has two sources. First, it gives the contribution from $0(\alpha_s)$ one-loop corrections to $e^+e^-\to q\bar{q}$, and second, at $\chi=+1$, it receives contributions of the form (2.18) from $e^+e^-\to q\bar{q}G$ events in which one of the final particles passes through both coincident detectors. The constants $C_{\pm 1}$ both diverge logarithmically as the infrared regulator (e.g., a fictitious gluon mass μ) is taken to zero. The coefficient C_{+1} of the delta function at $\chi=+1$ is given simply by the mean of F_2^{same} in (2.18):

$$C_{+1} = \left\langle \sum_i \frac{2E_i^2}{s}\right\rangle, \tag{2.28}$$

where the average encompasses both $q\bar{q}$ and $q\bar{q}G$ final states at $0(\alpha_s)$. The nonlinearity of the form (2.28) in the energies of the final particles means that in averaging over possible final state configurations, collinear pairs of particles will be weighted differently from single particles which carry the sum of their momenta. For this reason, the collinear divergences from $q\bar{q}$ and $q\bar{q}G$

final states will not cancel in (2.28), and C_{+1} will diverge like $\log(s/\mu^2)$ as μ^2 goes to zero. One finds, in fact, that ($\beta=\mu^2/s$ and $\zeta(2)=\pi^2/6$)

$$C_{+1} \simeq \frac{\alpha_s}{\pi}\left[\log(\beta)+\frac{77}{18}\right] \tag{2.29}$$
$$\left(+\frac{2\alpha_s\beta}{9\pi}[6\log^2(\beta)+21\log(\beta)-12\zeta(2)-41]+0(\beta^2)\right).$$

However, the integral over χ of the second term in (2.24) (regularized by the introduction of a finite β) for $\langle F_2^{pt}(\chi)\rangle$, which arises from $q\bar{q}G$ final states, also has a logarithmic divergence in β close to $\chi=+1$. This divergence cancels against C_{+1} when $\langle F_2^{pt}(\chi)\rangle$ is integrated over χ with a (non-singular) weight function, such as $P_l(\chi)$. This is, of course, necessary in order that the $\langle H_l\rangle$ obtained from $\langle F_2^{pt}(\chi)\rangle$ using (1.4) should be infrared finite as $\mu\to 0$. Note that if detectors of finite area are considered, then $\langle F_2^{pt}(\chi)\rangle$ is smeared according to (2.10); the resulting $\langle F_2(\chi;\delta)\rangle$ is finite at all χ, but diverges at $\chi=1$ like $\log(1-\delta)$ [to $0(\alpha_s)$] as the detector size is taken to zero.

The coefficient of the $0(\alpha_s)$ delta function in the backward direction ($\chi=-1$) in (2.24) is given by

$$C_{-1}=\left\langle\sum_i \frac{2E_iE_{i'}}{s}\right\rangle, \tag{2.30}$$

where i' is a particle exactly back-to-back with i. This receives contributions only from loop corrections to $e^+e^-\to q\bar{q}$; in fact, it is simply the total cross-section for the process $e^+e^-\to q\bar{q}$ (or, equivalently, the quark electromagnetic form factor)[7]:

$$C_{-1}\simeq\frac{-2\alpha_s}{3\pi}\left[\log^2(\beta)+\frac{3}{2}\log(\beta)-\frac{7}{2}++\zeta(2)\right] \tag{2.31}$$
$$\left(+\frac{4\alpha_s\beta}{3\pi}[\log^2(\beta)+\log(\beta)-1-2\zeta(2)]+0(\beta^2)\right).$$

7 Note that the form depends critically on the method of infrared regularization. If, instead of retaining a finite gluon mass, we had kept the quark off shell by an amount $\sqrt{\gamma s}$, then the kinematic limits change, and roughly β is replaced by $\sqrt{\gamma}$ so that the form of (3.9) is modified, becoming

$$C_{-1}\simeq\frac{2\alpha_s}{3\pi}[-2\log^2\gamma-3\log\gamma+8\zeta(2)-1].$$

For on-shell fermions of mass $\sqrt{\gamma s}$, a finite β must be retained to regularize soft divergences and

$$C_{-1}\simeq\frac{2\alpha_s}{3\pi}[-\log^2\gamma-4\log\beta\log\gamma-4\log\gamma+8\zeta(2)-5/2].$$

The double logarithmic terms in, for example, Eq. (2.31) can be summed to all orders in α_s to obtain a leading log estimate for the quark form factor. The estimate will be dual (as by the usual inclusive-exclusive connection) to results for quark fragmentation functions close to $x=1$. The dependence of the form factor on the infrared regularization procedure will be manifest in the various ways in which the limit $x\to 1$ is taken for the fragmentation function

Once again, in integrals of $\langle F_2^{pt}(\chi)\rangle$, these divergences are canceled by corresponding divergences in integrals of the $q\bar{q}G$ contribution (2.25) to $\langle F_2^{pt}(\chi)\rangle$ around $\chi=-1$. The presence of a $\log^2$ divergence in the individual terms around $\chi=-1$ is a consequence of the fact that a $q\bar{q}G$ final state becomes indistinguishable from $q\bar{q}$ if either one of the particles becomes soft or a pair of them are collinear. The introduction of a finite quark mass regularizes the collinear divergences to $0(\alpha_s)$, so that C_{+1} would then exhibit no divergence. However, a single log divergence would remain in C_{-1}, which could be regularized by taking a finite gluon mass (see Footnote 7).

Divergences are present in $F_2^{pt}(\chi)$ at a given order in α_s, at any value of χ for which $F_2^{pt}(\chi)$ is non-vanishing in lower orders. At $0(\alpha_s)$, $e^+e^-\to q\bar{q}(G)$ gives divergences only at $\chi=\pm 1$, where $\langle F_2^{pt}(\chi)\rangle$ for $e^+e^-\to q\bar{q}$ is non-vanishing. As described above, these divergences cancel against those from one-loop corrections to $e^+e^-\to q\bar{q}$ when $F_2^{pt}(\chi)$ is smeared (e.g., by consideration of detectors with finite area). In higher orders, $\langle F_2^{pt}(\chi)\rangle$ exhibits compensating divergences at each value of χ: it must be considered a generalized function, meaningful only when smeared in χ. This effect also afflicts the distributions in the H_l: the $\langle H_l\rangle$ are, however, genuinely infrared stable; their construction from $\langle F_2^{pt}(\chi)\rangle$ via (1.4) effects the necessary averaging. The divergences in $\langle F_2^{pt}(\chi)\rangle$ render it potentially more sensitive to hadronization corrections: the formation of hadrons introduces a presently unknown smearing. The distribution of events in $F_2(\chi)$, $1/\sigma\, d\sigma/dF_2(\chi)$ is, as described below, extremely sensitive to unknown details of fragmentation. [The divergences which cancel in $\langle F_2(\chi)\rangle$ when smeared over small ranges in χ appear as separated divergent peaks in the distribution in $F_2(\chi)$.]

2.3. *Heavy Resonance Decay $\zeta\to GGG$*

The decay $\zeta\to GGG$ of a heavy $^3S_1\, Q\bar{Q}$ resonance gives

$$\langle F_2^{pt}(\chi)\rangle=\left(\frac{6}{\pi^2-9}\right)\frac{1}{(1-\chi)^3}\left\{(2-5\chi)\sqrt{1-\chi^2}\left(\frac{\cos^{-1}\chi}{2}\right)\right.$$
$$\left.-(3\chi^2+4\chi+5)\log\left(\frac{1+\chi}{2}\right)+(1-\chi)(2\chi-5)\right\}$$
$$+\left(\frac{13\pi^2-127}{2(\pi^2-9)}\right)\delta(1-\chi), \tag{2.32}$$

where the last term comes from events in which the same particle passes through both detectors. At $\chi=0$ one finds

$$\langle F_2^{pt}(0)\rangle=\left(\frac{6}{\pi^2-9}\right)[5(\log 2-1)+\frac{\pi}{2}]\simeq 0.252. \tag{2.33}$$

Near $\chi=-1$, (2.32) becomes

$$-\frac{3}{2(\pi^2-9)}\left[\log\left(\frac{1+\chi}{2}\right)+7+\ldots\right], \tag{2.34}$$

while at $\chi=+1$, the regular part of (2.32) tends to $1/(10(\pi^2-9))\simeq 0.114$.

The differential cross-section for $\zeta\to GGG$ is barely distinguishable from uniform in three-body phase space, which would give

$$\langle F_2^{pt}(\chi)\rangle=\frac{24}{(\chi-1)^5}\left\{(\chi^2+10\chi+13)\log\left(\frac{1+\chi}{2}\right)+3(1-\chi)(\chi+3)\right\}+\tfrac{3}{4}\delta(1-\chi), \tag{2.35}$$

$$\langle F_2^{pt}(0)\rangle=24(13\log 2-9)\simeq 0.26.$$

Near $\chi=-1$, $\langle F_2^{pt}(\chi)\rangle$ in this case becomes

$$-3\left[\log\left(\frac{1+\chi}{2}\right)+3+\ldots\right]. \tag{2.36}$$

This integrable divergence has its origins in the Jacobian from the differential cross-section in (x_1, x_2) to that in (x_1, χ). Near $\chi=+1$, the regular part of $\langle F_2^{pt}(\chi)\rangle$ tends to 1/10. When a phase-space generated final state contains more than three particles, the Jacobian divergence at $\chi=-1$ visible in (2.36) [and which becomes $\delta(1+\chi)$ for a two-particle final state] disappears. This occurs even for the rather constrained 6 particle final state discussed in Sect. 2.5 (2.39). $\langle F_2^{pt}(\chi)\rangle$ becomes progressively flatter as the multiplicity of the final state increases and for a truly isotropic final state containing an infinite number of particles, $F_2^{pt}(\chi)=1$. [It is a general feature of QCD processes that the structure of events at the lowest contributing order in α_s is usually well-approximated by distributing the final state particles uniformly in the available phase space (appropriate for their multiplicity). In higher orders, infrared divergences tend to concentrate further emissions into jets along the directions of the partons at lowest order, thereby approximately preserving the lowest order shape, at least on large angular scales[8].

2.4. $\langle F_2\rangle$ and $1/\sigma\, d\sigma/dF_2$ for Hadronic Two- and Three-Jet Events

In this section we estimate the energy correlations to be expected in hadronic events arising from the processes $e^+e^-\to q\bar{q}(G)$ and $e^+e^-\to\zeta\to GGG$. We also give estimates for the uncorrected process $e^+e^-\to q\bar{q}$ which would occur alone if $\alpha_s=0$. To account for fragmentation of quarks and gluons into hadrons, we use the phenomenological model developed by Field and Feynman [6]. For $q\bar{q}(G)$ final states, we use the somewhat ad hoc prescription introduced in [1], and used successfully in analyses of data from PETRA [7].

8 The $\langle H_l\rangle$ for a process are therefore typically well approximated by distributing the partons in the lowest-order final state uniformly in phase space. For two-particle final states, only one point in phase space is, of course, allowed and, as usual, $H_l=0(1)$ for l odd (even). [The processes $e^+e^-\to q\bar{q}(GG\ldots)$ usually lead to two jets and, therefore, roughly preserve the lowest-order results for the $\langle H_l\rangle$. However, as l increases, the $\langle H_l\rangle$ become progressively more sensitive to the detailed structure of the events and probe the internal constitution of the jets so that the lowest order structure is lost.] For three-particle events, a phase space distribution gives

$$\langle H_2\rangle=(3\pi^2-29)\simeq 0.61$$

$$\langle H_3\rangle=(75\pi^2-740)\simeq 0.22$$

$$\langle H_\infty\rangle=3/8=0.375.$$

Note the extreme similarly between these results and those for $\zeta\to GGG$ at lowest order ($\langle H_2\rangle\simeq 0.62$, $\langle H_3\rangle\simeq 0.22$, $\langle H_\infty\rangle\simeq 0.3751$). In higher orders of α_s, the $\langle H_l\rangle$ for large l again deviate significantly from the lowest-order results or from the phase space approximation to them. For an n particle final state distributed uniformly in phase space, the $\langle H_l\rangle$ are approximately $1/n$ so that as $n\to\infty$, the usual result $\langle H_l\rangle=0$ $(l\neq 0)$ for a genuinely isotropic system is regained

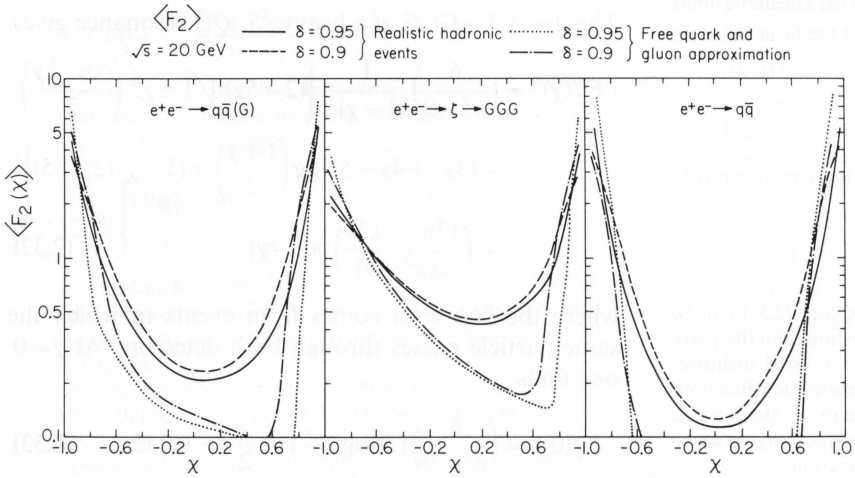

Fig. 3. A comparison at $\sqrt{s}=20$ GeV of the mean value of the energy correlation F_2 for two different detector sizes given by $\delta=0.9$ or $\delta=0.95$ (corresponding to detectors of half-angle 26° and 18°, respectively)

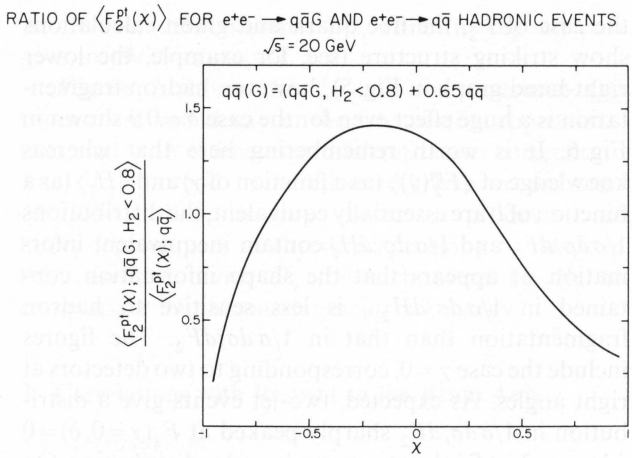

Fig. 4. The ratio of the mean energy correlation between point detectors $\langle F_2^{pt}(\chi)\rangle \equiv \langle F_2(\chi;\delta=1)\rangle$ for hadrons produced by the processes $e^+e^- \to q\bar{q}G$ and $e^+e^- \to q\bar{q}$ at $\sqrt{s}=20$ GeV. Note that at this energy, our prescription for treating fragmentation takes 65% of $q\bar{q}(G)$ final states to contain two jets and, therefore, to evolve roughly like $q\bar{q}$ final states

Our method consists in generating true three-jet events when the $q\bar{q}G$ produced in the subprocess satisfy the cut $H_2<0.8$, and two jet events otherwise in such a way as to give the correct total $0(g^2)$ cross-section: $\simeq \sigma_0(1+\alpha_s/\pi)$. The cut on H_2 represents the resolution of the hadron final state to changes in the subprocess final state: the hadrons do not reflect the presence of the extra gluon if its transverse momentum is too small.

In Figs. 2 and 3 we show estimates of $\langle F_2(\chi;\delta)\rangle$ with $\delta=0.95$ (18° detectors) and $\delta=0.9$ (26° detectors) for hadronic events, and in the free parton approximation. At sufficiently high energies, hadronization effects must disappear, but Figs. 2 and 3 show that they are still present in the PETRA, PEP energy range $20 \lesssim \sqrt{s} \lesssim 40$ GeV. The effects are rather less severe for the $1/\sigma\, d\sigma/dH_l$ ($l_s=2,3$) discussed in [1]. The results for hadronic events in Fig. 3 with $\delta=0.9$ are slightly closer to the free parton approximation than those with $\delta=0.95$: the small difference indicates that hadroni-

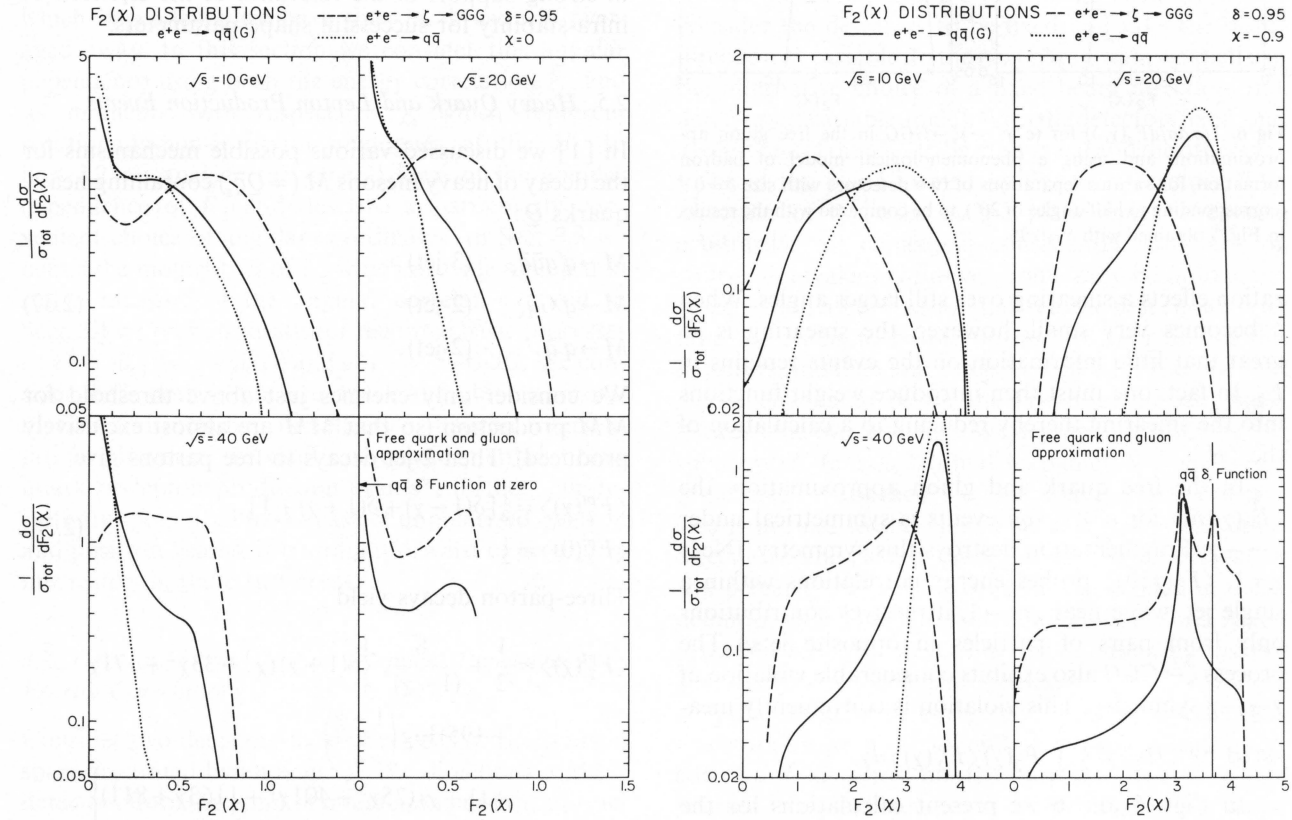

Fig. 5. The distributions $1/\sigma\, d\sigma/dF_2(\chi,\delta)$ calculated for various separations χ of two detectors with size $\delta=0.95$ ($\cong 18°$) resulting from the processes $e^+e^- \to q\bar{q}$, GGG, and $q\bar{q}(G)$. Calculations in the free quark and gluon approximation are shown as well as those obtained from an estimate of the effects of fragmentation to hadrons at $\sqrt{s}=10$, 20, and 40 GeV. In the free quark approximation $e^+e^- \to q\bar{q}$ gives a delta function contribution, smeared to angles $\chi=\pm(2\delta^2-1)$ by the finite detector sizes. The curve marked $q\bar{q}(G)$ in the free quark and gluon approximation is $q\bar{q}G$ with an $H_2<0.8$ cut but without the $q\bar{q}$ (delta function) term added

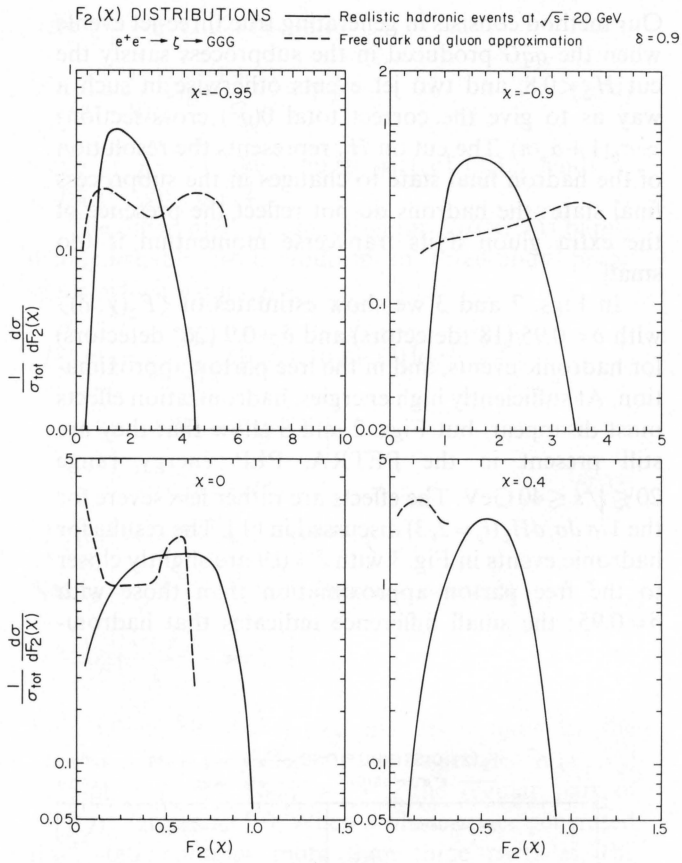

Fig. 6. $1/\sigma\, d\sigma/dF_2(\chi,\delta)$ for $(e^+e^-\to)\zeta\to GGG$ in the free gluon approximation, and using a phenomenological model of hadron formation, for various separations of two detectors with size $\delta=0.9$ (corresponding to half-angles of 26°), to be compared with the results in Fig. 5 obtained with $\delta=0.95$

zation effects a smearing over still larger angles. When δ becomes very small, however, the smearing is so great that little information on the events remains in F_2. In fact, one must then introduce weight functions into the smearing thereby reducing to a calculation of the $\langle H_l\rangle$.

In the free quark and gluon approximation, the $\langle F_2(\chi;\delta)\rangle$ for $e^+e^-\to q\bar{q}$ events is symmetrical under $\chi\to-\chi$. Fragmentation destroys this symmetry. (Near $\chi=1$, $\langle F_2(\chi;\delta)\rangle$ probes energy correlations within a single jet, while near $\chi=-1$, it receives contributions only from pairs of particles in opposite jets.) The process $\zeta\to GGG$ also exhibits considerable violation of $\chi\to-\chi$ symmetry. This violation is conveniently measured by $\langle H_3\rangle=\frac{1}{2}\int_{-1}^{1} P_3(\chi)\langle F_2^{pt}(\chi)\rangle\, d\chi$.

In Figs. 5 and 6 we present calculations for the distributions $1/\sigma\, d\sigma/dF_2$. These are rather disappointing. In our study of the H_l [1], we found that the distributions $1/\sigma\, d\sigma/dH_l$ (at least for $l=2$ and 3) were not seriously affected by hadron fragmentation and provided very distinctive tests of the basic dynamics. In the case of F_2, the free quark and gluon calculations show striking structure (see, for example, the lower right-hand graph in Fig. 5); however, hadron fragmentation is a huge effect even for the case $\delta=0.9$ shown in Fig. 6. It is worth remembering here that whereas knowledge of $\langle F_2^{pt}(\chi)\rangle$ (as a function of χ) and $\langle H_l\rangle$ (as a function of l) are essentially equivalent, the distributions $1/\sigma\, d\sigma/dF_2$ and $1/\sigma\, d\sigma/dH_l$ contain inequivalent information. It appears that the shape information contained in $1/\sigma\, d\sigma/dH_{2,3}$ is less sensitive to hadron fragmentation than that in $1/\sigma\, d\sigma/dF_2$. The figures include the case $\chi=0$, corresponding to two detectors at right angles. As expected, two-jet events give a distribution in $1/\sigma\, d\sigma/dF_2$ sharply peaked at $F_2(\chi=0,\delta)=0$ whereas 3 jet final states give a broader distribution. On comparing $e^+e^-\to\zeta\to GGG$ and $e^+e^-\to q\bar{q}(G)$, one sees that the former gives many more events with large values of $F_2(\chi=0,\delta)$. This behavior is qualitatively as expected and should be preserved regardless of how one treats the hadron fragmentation. Note that the extreme sensitivity of $1/\sigma\, d\sigma/dF_2$ to fragmentation is to be expected because of the infrared instability of F_2. The inadequacy of $1/\sigma\, d\sigma/dF_2$ compared to $1/\sigma\, d\sigma/dH_{2,3}$ is in strong support of the relevance of the criterion of infra-stability for successful shape parameters.

2.5. Heavy Quark and Lepton Production Events

In [1] we discussed various possible mechanisms for the decay of heavy mesons M $(=Q\bar{q}_s)$ containing heavy quarks Q:

$$\begin{aligned} &M\to q'q\bar{q}\bar{q}_s && \text{(3-jet)}\\ &M\to q'G\bar{q}_s && \text{(2-jet)}\\ &M\to q'\bar{q} && \text{(2-jet)}. \end{aligned} \tag{2.37}$$

We consider only energies just above threshold for $M\bar{M}$ production (so that $M\bar{M}$ are almost exclusively produced). Then 2-jet decays to free partons give

$$\begin{aligned} &\langle F_2^{pt}(\chi)\rangle=\tfrac{1}{2}[\delta(1-\chi)+\delta(1+\chi)+1],\\ &\langle F_2^{pt}(0)\rangle=\tfrac{1}{2}. \end{aligned} \tag{2.38}$$

Three-parton decays yield

$$\begin{aligned} \langle F_2^{pt}(\chi)\rangle=\frac{1}{2}+\frac{8}{(1-\chi)^7}\Big\{&6(1+\chi)(\chi^3+33\chi^2+171\chi\\ &+195)\log\left(\frac{1+\chi}{2}\right)\\ &+(1-\chi)(25\chi^3+401\chi^2+1163\chi+811)\Big\}\\ &+\frac{11}{30}\delta(1-\chi), \end{aligned} \tag{2.39}$$

so that

$$\langle F_2^{pt}(0)\rangle=\tfrac{1}{2}+8(811-1170\log 2)\simeq 0.642. \tag{2.40}$$

At $\chi = -1$, (2.39) becomes 7/2, while the regular part goes to 19/35 as $\chi \to +1$.

Figure 7 shows the $\langle F_2(\chi)\rangle$ for threshold $Q\bar{Q}$ production and decay in the free parton approximation, and with estimates of hadronization corrections. The $\langle F_2(\chi)\rangle$ tend to be close to the isotropic limit $\langle F_2(\chi)\rangle = 1$. We also give results for production of heavy lepton pairs at threshold decaying to $u\bar{d}\nu_L$; in this case, we divide F_2 for each event by H_0 to compensate for the missing neutrino energy.

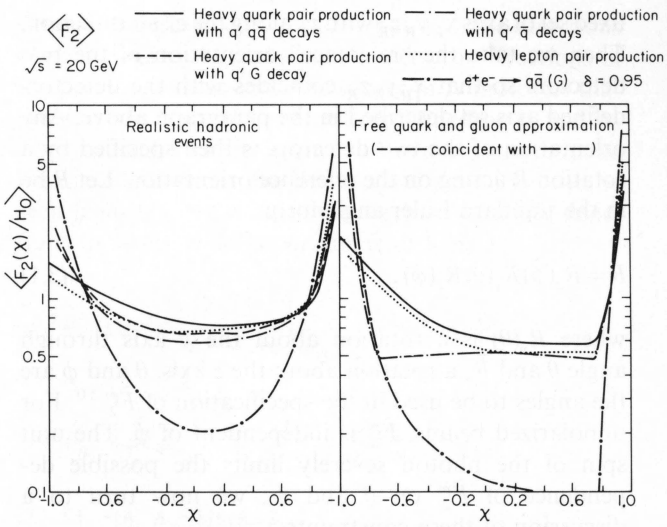

Fig. 7. The mean energy correlation function $\langle F_2(\chi,\delta)\rangle$ for events containing heavy quark or lepton production with various mechanisms for heavy meson decay. For comparison, we show results for the continuum reaction $e^+e^- \to q\bar{q}(G)$ from Fig. 2

3. Correlations with Respect to the Beam Axis

3.1. Introduction

We have discussed above the rotationally invariant observable $F_2(\chi;\delta)$ obtained by averaging $\tilde{F}_2$, defined in (1.2), over all possible positions of the two detectors which preserve their relative orientation. This averaged $F_2(\chi;\delta)$ characterizes the shapes of events and is probably the most direct probe of their dynamical mechanisms. However, QCD also makes unambiguous predictions for the dependence of the shapes of events on their orientation with respect to the beam axis, which dependence we have thus far brusquely averaged away. In this section we consider this angular dependence using both the energy correlation $\tilde{F}_2$ and its moments with respect to χ, which represent rotationally-non-invariant analogues of the H_l. In Sect. 3.2 we analyze the general form of the angular dependence of $\tilde{F}_2$ and describe a particularly convenient choice of angular coordinates. In Sect. 3.3 we define the moments Ξ of $\tilde{F}_2$ which provide an infrared stable measure of the angular correlations, and in Sect. 3.4 we present results for the three basic processes $e^+e^- \to q\bar{q}$, $e^+e^- \to q\bar{q}(G)$ and $e^+e^- \to \zeta \to GGG$. We consider these both in the free quark and gluon approximation and including the effects of hadron fragmentation. However, we shall not consider either heavy quark or lepton production events[9]; further, our results are specialized to the case of unpolarized electron and positron beams. It is straightforward to generalize our results in these two areas.

3.2. General Form of the Angular Dependence of Energy Correlations

Consider two detectors fixed at particular positions in space separated by an angle χ. The directions of these detectors from the point of interaction (and the normal to the plane defined by them) may be used to define an orthogonal set of axes xyz with respect to which one can specify the direction of the beam axis. Temporarily we consider the detectors to be fixed and take the beam direction as variable. In the next paragraph, we shall use the alternative choice of a fixed beam direction and detectors at variable angles. With the detectors fixed, one assigns one of the axes to be the normal and the other two to be in the plane formed by the two detectors. The direction of the axes in the plane may be chosen arbitrarily. All choices, if consistently used, are, of course, equivalent; however, some may be more convenient than others. As we shall see, the best choice is to take the z axis to be the normal to the plane of the detectors, and the x and y axes to be in the plane, with the x axis defined to be on the line bisecting the angle between the two detectors. We denote this choice by the subscript N (z axis Normal to plane). We shall also sometimes discuss the P system (z axis in Plane) whose y axis is normal to the plane and z axis is in the same direction as the x axis in the N system. The careful reader will perceive that various signs are undefined in these definitions (e.g., one can reverse directions of z and y axes in the N system). However, no parity-conserving observable is sensitive to the ambiguities.

Now consider the energy correlations between two detectors for an e^+e^- annihilation event. Clearly, the correlation depends on the direction of the beam referred to the axis sets we described above; this beam direction may be specified by spherical polar angles (θ', ϕ') and so we are led to define a beam-orientated energy correlation $\tilde{F}_2^{pt}$ that is a function of χ, δ, θ' and ϕ'. To be precise, we shall actually not define θ', ϕ' exactly in this way but rather fix the e^+e^- direction and define a

9 For heavy meson pair production near threshold, the spinless nature of the mesons prevents any angular dependence of energy correlations, but for spin $-\frac{1}{2}$ heavy lepton pair production, there should be a definite non-trivial angular dependence

fixed set of axes $x_R y_R z_R$ with z_R along the e^+e^- direction. Then we take the "reference" orientation of the two detectors so that $x_R y_R z_R$ coincides with the detector-defined axis set described in the paragraph above. Any orientation of the two detectors is then specified by a rotation R acting on the reference orientation. Let R be in the standard Euler angle form

$$R = \hat{R}_z(\tilde{\phi})\hat{R}_y(\theta)\hat{R}_z(\phi), \tag{3.1}$$

where $\hat{R}_y(\theta)$ is a rotation about the y axis through angle θ and $\hat{R}_z$ a rotation about the z axis. θ and ϕ are the angles to be used in the specification of $\tilde{F}_2^{pt}$ [10]. For unpolarized beams, $\tilde{F}_2^{pt}$ is independent of $\tilde{\phi}$. The unit spin of the photon severely limits the possible dependence of $\tilde{F}_2^{pt}$ on θ and ϕ; we now turn to a discussion of these constraints.

Consider the general process

$$e^+e^- \to 1+2+\text{anything}, \tag{3.2}$$

where we have specialized to the case of point detectors and consider 1 and 2 as particles heading in the directions of the two detectors. Working in the virtual photon rest frame, let λ be the spin component of the virtual photon referred to the e^+e^- direction as a quantization axis, and let μ be the spin component of the virtual photon with respect to the "reference" final state axes. Then if α denotes the unmeasured momenta and helicities of the final particles, the amplitude for $e^+e^- \to \gamma^* \to 1+2+\text{anything}$ may be written as

$$A_{\lambda\alpha} = \sum_\mu G_\lambda d^1_{\lambda\mu}(\theta)\exp(-i\mu\phi)H_{\mu\alpha}, \tag{3.3}$$

where G_λ, $H_{\mu\alpha}$ are vertex functions, which give the helicity amplitudes for $e^+e^- \to \gamma^*$ and $\gamma^* \to 1+2+\text{anything}$, respectively. Taking $H_{1\alpha} = a_\alpha$, $H_{0\alpha} = b_\alpha$, $H_{-1\alpha} = c_\alpha$, and using $G_1 = -G_{-1}$, $G_0 = 0$ (for massless $e^\pm$), the square of the amplitude (3.3) becomes

$$\begin{aligned}\frac{d^2\sigma}{d(\cos\theta)d\phi} \propto \sum_\alpha \{&|d^1_{11}(\theta)e^{-i\phi}a_\alpha + d^1_{10}(\theta)b_\alpha \\ &+ d^1_{1-1}(\theta)e^{i\phi}c_\alpha|^2 \\ &+ |d^1_{-11}(\theta)e^{-i\phi}a_\alpha + d^1_{-10}(\theta)b_\alpha \\ &+ d^1_{-1-1}(\theta)e^{i\phi}c_\alpha|^2\},\end{aligned} \tag{3.4}$$

which gives the inclusive cross-section $e^+e^- \to 1+2+\text{anything}$. For point detectors, one must simply multiply it by $\frac{E_1E_2}{s}$ to obtain $\tilde{F}_2^{pt}(\chi,\theta,\phi)$. One may expand the resulting expression and derive the general form for the θ and ϕ dependence of $\tilde{F}_2^{pt}$. The parity invariance of the interaction places some constraints on this form. The constraints take a different form depending on whether the z axis lies in the 12 plane (as in the P system) or along the normal to it (N system). In a P-type system, parity invariance implies

$$\left.\begin{aligned} b_\alpha &= \eta_\alpha b_{-\alpha} \\ a_\alpha &= -\eta_\alpha c_{-\alpha}\end{aligned}\right\} z \text{ axis in 12 plane}, \tag{3.5}$$

where $\eta_\alpha = \pm 1$ is some phase and $-\alpha$ denotes the state obtained by application to α of the symmetry operator $S = P\hat{R}_y(\pi)$ [P = parity operator, $\hat{R}_y(\pi)$ a rotation through π about the y direction]. S, of course, leaves the directions of 1 and 2 invariant. Combining (3.5) and (3.4), one finds

$$\begin{aligned}\frac{d^2\sigma}{d\cos\theta_P d\phi_P} &= A_P(1+\cos^2\theta_P) + B_P\sin^2\theta_P \\ &\quad + C_P\sin^2\theta_P\cos 2\phi_P + D_P\sin 2\theta_P\cos\phi_P,\end{aligned} \tag{3.6}$$

where A_P through D_P (which, of course, depend on χ) can be related to bilinear sums over a_α, b_α, and c_α.

If now the z axis is taken along the normal to the 12 plane, the symmetry operator for the system becomes $S = P\hat{R}_z(\pi)$, so that the constraints from parity invariance become

$$\left.\begin{aligned} a_\alpha &= -\eta_\alpha a_\alpha \\ c_\alpha &= -\eta_\alpha c_\alpha \\ b_\alpha &= \eta_\alpha b_\alpha\end{aligned}\right\} z \text{ axis along normal to 12 plane}. \tag{3.7}$$

Combining (3.7) and (3.4), one finds

$$\begin{aligned}\frac{d^2\sigma}{d\cos\theta_N d\phi_N} &= A_N(1+\cos^2\theta_N) + B_N\sin^2\theta_N \\ &\quad + C_N\sin^2\theta_N\cos 2\phi_N \\ &\quad + D_N\sin 2\theta_N\sin 2\phi_N.\end{aligned} \tag{3.8}$$

Comparing (3.6) and (3.8), we see that there are, in general, 4 independent beam-oriented energy correlation functions. The specific expansion coefficients in the complete energy correlation as a function of the directions of the detectors with respect to the beam (or, equivalently, at least for the point detector case considered here, the inclusive differential cross-section for $e^+e^- \to \gamma^* \to 1+2+\text{anything}$) depend, however, on the choice of coordinate system. The results (3.6) and (3.8) hold for any choice of orthogonal axes in the 12 planes. However, they must be symmetric under the interachange $1 \leftrightarrow 2$. This constraint may be expressed most simply if one chooses one of the axes in the plane along the bisector of the angle between the directions of 1 and 2. In this case, the terms D_P and D_N vanish and one may write the angular distribution in either the N or P

10 $\theta' = -\theta$, $\phi' = -\phi$ relates this to previous description. In (3.9) one can use either choice as allowed transformation functions are independent of a sign change for θ and ϕ

system as

$$\frac{d^2\sigma}{d(\cos\theta)\,d\phi} \propto \langle \tilde{F}_2^{pt}(\chi,\theta,\phi)\rangle = T(\chi)\,\{1+J(\chi)P_2(\cos\theta) + K(\chi)\sin^2\theta\cos 2\phi\}\,. \tag{3.9}$$

With the above choice, our previous rotational averaged $\langle F_2(\chi)\rangle$ is just the function $T(\chi)$ while moments of $\tilde{F}_2^{pt}(\chi,\theta,\phi)$ with respect to the orthogonal functions $P_2(\cos\theta)$ and $\sin^2\theta\cos 2\phi$ give J and K:

$$\langle 1\rangle = \frac{1}{4\pi}\int d\Omega \langle \tilde{F}_2^{pt}(\chi,\theta,\phi)\rangle = T(\chi)$$

$$\langle P_2(\cos\theta)\rangle/\langle 1\rangle = J(\chi)/5 \tag{3.10}$$

$$\langle \sin^2\theta\cos 2\phi\rangle/\langle 1\rangle = 4K(\chi)/15\,.$$

3.3. Moments of Angular Correlations

The H_l observables discussed in [1] were of the form

$$\sum_{i,j}\frac{|\mathbf{p}_i|\,|\mathbf{p}_j|}{s}\,f(\hat{p}_i\cdot\hat{p}_j)\,, \tag{3.11}$$

where $\hat{p}_i$, $\hat{p}_j$ are unit vectors along the momenta of particles i and j and the f were chosen to be the Legendre polynomials. The H_l give a complete specification of the rotationally invariant two-point energy correlation function in an event. In [10] and in Sect. 3 below, we discuss the expansion of the three-point energy correlation defined as

$$\sum_{i,j,k}\frac{|\mathbf{p}_i|\,|\mathbf{p}_j|\,|\mathbf{p}_k|}{s^{3/2}}\,f(\hat{p}_i,\hat{p}_j,\hat{p}_k)\,. \tag{3.12}$$

In this section, we consider another extension of (3.11) in which f now depends on the direction of the incoming beams, $\hat{b}$. We take

$$\Xi_f = \sum_{i,j}\frac{|\mathbf{p}_i|\,|\mathbf{p}_j|}{s}\,f(\hat{b},\hat{p}_i,\hat{p}_j)\,. \tag{3.13}$$

We find that these observables provide information on the angular distributions of planar structures in events with respect to the beam direction.

The general analysis of Sect. 3.2 allows us to write and f in terms of the linearly independent functions

$$\begin{aligned} f_0^l &= \sin^2\phi_{ij}P_l(\cos\phi_{ij})\\ f_1^l &= \sin^2\phi_{ij}P_2(\cos\theta_{N_{ij}})P_l(\cos\phi_{ij})\\ f_2^l &= \sin^2\phi_{ij}\sin^2\theta_{N_{ij}}\cos 2\phi_{N_{ij}}P_l(\cos\phi_{ij})\,, \end{aligned} \tag{3.14}$$

where ϕ_{ij} is the angle between particles i and j. $\theta_{N_{ij}}$ and $\phi_{N_{ij}}$ are the angles which specify the beam direction in the N_{ij} coordinate system. This set of axes $\{xyz\}$ is defined as described in Sect. 3.2, but with the directions of particles i and j replacing the detector directions of the previous discussion. The subscript N indicates that the z axis is normal to the plane defined by $\hat{p}_i$ and $\hat{p}_j$. The explicit factor $\sin^2\phi_{ij}$ in (3.14) is necessary to make the f_i^l well defined in the limits $\phi_{ij}=0$ or π. This can be seen from the expressions for the beam angular functions in terms of scalar products of $\hat{b}$, $\hat{p}_i$, and $\hat{p}_j$:

$$\sin^2\theta_{N_{ij}}\cos^2\phi_{N_{ij}} = \frac{1}{4\cos^2\phi_{ij}/2}\,[b\cdot(\hat{p}_i+\hat{p}_j)]^2$$

$$\sin^2\theta_{N_{ij}}\sin^2\phi_{N_{ij}} = \frac{1}{4\sin^2\phi_{ij}/2}\,[\hat{b}\cdot(\hat{p}_i-\hat{p}_j)]^2\,, \tag{3.15}$$

$$\begin{aligned} f_0^l &= [1-(\hat{p}_i\cdot\hat{p}_j)^2]P_l(\hat{p}_i\cdot\hat{p}_j)\\ f_1^l &= [1-\tfrac{3}{2}((\hat{b}\cdot\hat{p}_i)^2+(\hat{b}\cdot\hat{p}_j)^2)\\ &\quad +3(\hat{b}\cdot\hat{p}_i)(\hat{p}_i\cdot\hat{p}_j)(\hat{p}_j\cdot\hat{b})]\,P_l(\hat{p}_i\cdot\hat{p}_j)\\ f_2^l &= [2(\hat{b}\cdot\hat{p}_i)(\hat{b}\cdot\hat{p}_j)-((\hat{b}\cdot p_i)^2\\ &\quad +(\hat{b}\cdot\hat{p}_j)^2)]\,P_l(\hat{p}_i\cdot\hat{p}_j)\,, \end{aligned} \tag{3.16}$$

which illustrates the necessity of the $\sin^2\phi_{ij}$ factor in the definition of f_k^l to avoid problems at $\phi_{ij}=0$ or π. We define Ξ_k^l using (3.13) with f_k^l as taken from (3.14) or (3.16). It is clear that the $\langle\Xi_k^l\rangle$ share the infrared stability of the $\langle H_l\rangle$ when they are computed in QCD perturbation theory.

Another possible set of observables, which appears to be less sensitive to hadron fragmentation than the Ξ_k^l (see below), is defined in analogy with (3.13):

$$\begin{aligned} \bar{\Xi}_k^l &= \sum_{i,j}\frac{|\mathbf{p}_i|\,|\mathbf{p}_j|}{s}\,\bar{f}_k^l(\hat{b},\hat{p}_i,\hat{p}_j)\\ \bar{f}_k^l &= f_k^l/(\sin^2\phi_{ij})\,. \end{aligned} \tag{3.17}$$

The $\bar{\Xi}_k^l$ are only independent of the Ξ_k^l for $l=0$ and 1. The definition (3.17) is singular at $\sin^2\phi_{ij}=0$, for $k=1$ or 2. For $\phi_{ij}=0$, the x axis remains well defined (along the $\hat{p}_i$, $\hat{p}_j$ direction) but the y and z axes of the N_{ij} system are undefined. In this case, we take the $\bar{f}_{1,2}^l$ to have the values obtained by averaging uniformly over all possible directions of the y and z axes in the plane perpendicular to $\hat{p}_i$, $\hat{p}_j$, so that

$$\begin{aligned} \bar{f}_1^l(\phi_{ij}=0) &= -\tfrac{1}{2}P_2(\cos\alpha_i)P_l(\cos\theta_{ij})\\ \bar{f}_2^l(\phi_{ij}=0) &= P_2(\cos\alpha_i)P_l(\cos\theta_{ij})\,, \end{aligned} \tag{3.18}$$

where α_i is angle between beam direction and the particles i or j.

In the case $\phi_{ij}=\pi$, an analogous situation pertains and only the y axis is well defined. We take $\bar{f}_{1,2}^l$ to have

the value obtained by averaging over all possible directions for the x and z directions, so that

$$\begin{aligned} \bar{f}_1^l(\phi_{ij}=\pi) &= -\tfrac{1}{2}P_2(\cos\alpha_i)P_l(\cos\theta_{ij}) \\ \bar{f}_2^l(\phi_{ij}=\pi) &= -P_2(\cos\alpha_i)P_l(\cos\theta_{ij}). \end{aligned} \tag{3.19}$$

Note that in both limits, $\bar{f}_{1,2}^l$ is proportional to $P_2(\cos\alpha_i)$, giving the only possible non-trivial dependence on α_i.

The $\bar{\Xi}_k^l$ cannot be written in a form analogous to the H_l from which their infrared stability would be evident. Their values depend, of course, on the treatment of the singular case $\sin\phi_{ij}=0$. We give evidence below that the prescription for this described above is correct and renders the $\bar{\Xi}_k^l$ infrared stable. It is clear that the energy weighting in (3.17) protects the $\bar{\Xi}_k^l$ from soft infrared divergences. Collinear quarks and gluons also give rise to divergences in the differential cross-section. The $\bar{\Xi}_k^l$ can only be infrared stable if they take on the same value for divergent configurations in which two separate particles are exactly collinear ($\phi_{ij}=0$) and in which a single particle carries their total momentum. This will be the case with our prescription for handling collinear particles only if, in configurations where the particles are nearly collinear, all potential divergences are independent of the azimuthal directions of the particles with respect to the axis defined by the vector sum of their momenta. Any dependence on the azimuthal direction will appear in the amplitude as terms proportional to $\gamma\cdot k_\perp$, where $k_\perp$ is the transverse momentum of one of the particles with respect to the total momentum axis. Divergences in the amplitude are (up to logarithms) of the form $dk_\perp/k_\perp$. Hence, any contribution to the amplitude which is not independent of azimuthal angle will be finite as $k_\perp\to 0$. Thus the divergent parts of amplitudes for collinear production of particles are azimuthally-symmetrical, so that (with our prescription) the $\bar{\Xi}_k^l$ take on the same value for this configuration as when a single particle is produced in place of several collinear ones. Hence it appears that the moments of the $\bar{\Xi}_k^l$ should be infrared stable when computed in QCD perturbation theory.

Consider now an event in which three partons are produced. Then the angular distribution of the plane defined by their momenta with respect to the beam axis will be characterized by $\Xi_{1,2}^l/\Xi_0^l$ or $\bar{\Xi}_{1,2}^l/\bar{\Xi}_0^l$. In actual events, where the final state consists of hadrons, the values of these ratios will approach the free quark and gluon results as $\sqrt{s}$ increases. The $\overset{\odot}{\Xi}{}_k^l$ therefore provide a method for determining the angular distributions of planes of particles with respect to the beam direction without requiring the plane to be found by minimizing an observable [8], which might well induce spurious effects. The $\overset{\odot}{\Xi}{}_k^l$ give the moments of the angular distributions of planes just as the B_l described in [2] describe the angular distributions of jets.

The angular distributions of planes in general depend both on their polar (θ) and azimuthal (ϕ) angles with respect to the beam direction. The polar and azimuthal dependences can, of course, be rearranged by making different choices of frame (e.g., N or P). One might expect that in some frame two jet events should contribute on average only to the polar distribution. However, while this is clearly the case for pure $q\bar{q}$ final states, it is no longer possible after fragmentation to hadrons to choose a frame in which the azimuthal dependence vanishes. Hence both $\overset{\odot}{\Xi}{}_1^l$ and $\overset{\odot}{\Xi}{}_2^l$ should be considered; no particular feature of the angular distribution appears to be especially distinguished.

Finally we note that $\overset{\odot}{\Xi}{}_k^l$ are the Legendre transforms (with respect to χ) of the angular terms (3.10) in the energy correlation function $\tilde{F}_2^{pt}$. Their relation to $\tilde{F}_2^{pt}$ is, therefore, analogous to the relation of the H_l to the rotationally-averaged F_2^{pt}.

3.4. *Some Analytical Results for $\tilde{F}_2^{pt}$*

For the process $e^+e^-\to q\bar{q}$, $\tilde{F}_2^{pt}(\chi,\theta,\phi)$ is only nonzero at $\chi=\pm 1$ where the "plane" given by the two detectors is undefined. We use the same azimuthally symmetric prescription for defining the plane here as we described for $\bar{\Xi}_k^l$ at $\sin\phi_{ij}=0$ in the previous section. If α is the angle between the e^+e^- and $q\bar{q}$ direction, then the $\frac{3}{8}(1+\cos^2\alpha)=\frac{1}{2}+\frac{1}{4}P_2(\cos\alpha)$ angular distribution gives for the parameters in $\tilde{F}_2^{pt}$ defined according to (3.10)

$$\begin{aligned} T(\chi) &= \delta(\chi-1)+\delta(\chi+1) \\ J(1) &= J(-1) = -\tfrac{1}{4} \\ K(1) &= -K(-1) = \tfrac{3}{2}. \end{aligned} \tag{3.20}$$

To estimate the modifications to our results when the q and $\bar{q}$ fragment into hadrons, we would usually simulate complete hadronic events. We do this in the next section but present here a simple estimate for the effects of fragmentation of $J(\chi)$ and $K(\chi)$ which agrees closely with the results from the more complicated model. Our simple estimate is obtained by assuming that $\tilde{F}_2(\chi)$ away from $\chi=\pm 1$ is dominated by a complete jet entering one detector and a single hadron from the other jet being incident on the second detector. The first jet then has an angular distribution $(1+\cos^2\alpha)$ with respect to the beam direction, while we take the single hadron to be distributed uniformly in azimuth about the direction of the jet from which it came. This picture leads to the simple predictions

$$\begin{aligned} J_{q\bar{q}\,\text{fragmentation}}(\chi) &\equiv -\tfrac{1}{4} \\ K_{q\bar{q}\,\text{fragmentation}}(\chi) &= \tfrac{3}{8}\chi \end{aligned} \tag{3.21}$$

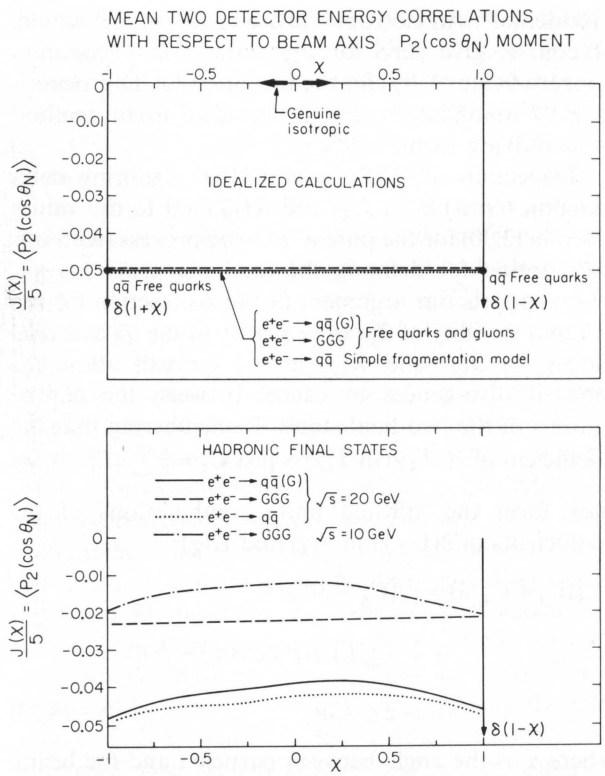

Fig. 8. The beam angular correlation $J(\chi)/5 = \langle P_2(\cos\theta_N)\rangle$ defined in (3.10) for the processes $e^+e^- \to q\bar{q}$, $e^+e^- \to q\bar{q}(G)$, and $\zeta \to GGG$, in the free quark and gluon approximation ("idealized calculation") and for simulated hadronic final states. We also show results for $e^+e^- \to q\bar{q}$ events obtained from the simple fragmentation model described in Sect. 3.4. There is a severe nonuniformity in the curves near $\chi = +1$, as discussed at the end of Sect. 3.4 [cf., (3.22)]. The figures do not attempt to illustrate this phenomenon correctly

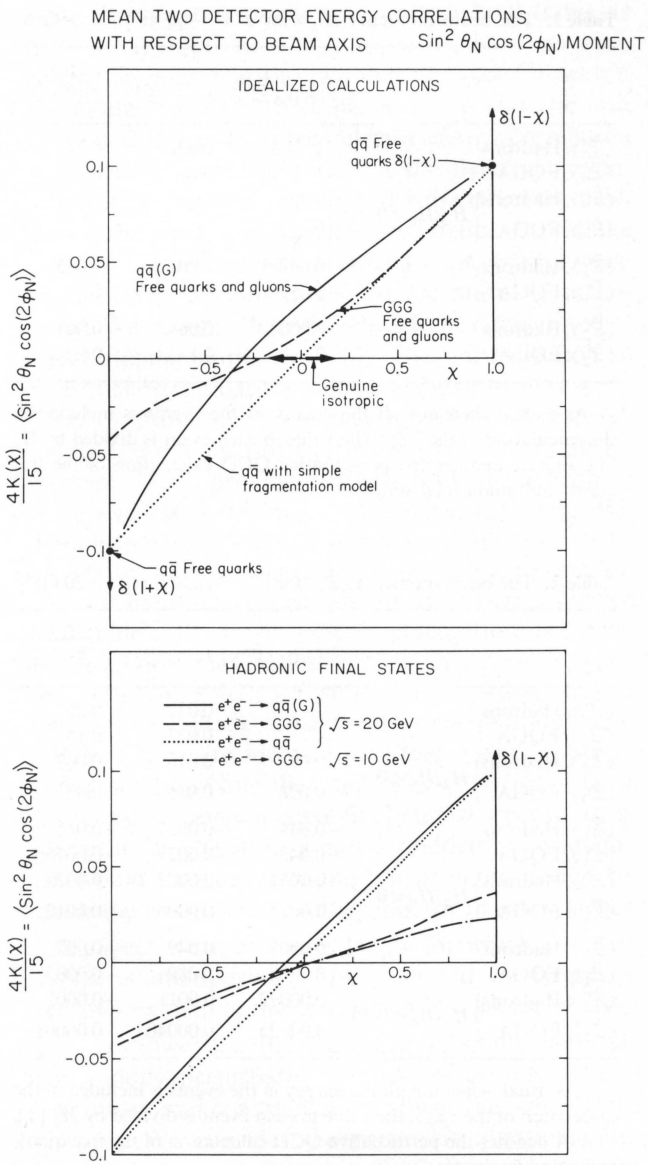

Fig. 9. The second independent beam angular correlation $4K(\chi)/15 = \langle \sin^2\theta_N \cos 2\phi_N\rangle$ for the same processes as given in Fig. 8. For both $J(\chi)$ and $K(\chi)$, the subscript N on the angles denotes the use of the frame where the z axis is perpendicular to plane defined by the two particles

which are in remarkably good agreement with the full Monte Carlo simulation of $q\bar{q}$ fragmentation shown in Figs. 8 and 9. Of course, this simple picture predicts only the angular correlations $J, K(\chi)$ and not the overall normalization $T(\chi)$.

For $e^+e^- \to q\bar{q}G$, the function $T(\chi) \equiv \langle F_2^{pt}(\chi)\rangle$ is given in (2.24). One can also calculate $J(\chi)$ and $K(\chi)$ in the free quark and gluon approximation to find [at $0(\alpha_s)$]

$$T_{q\bar{q}G}(\chi) J_{q\bar{q}G}(\chi) \equiv \frac{-T_{q\bar{q}G}(\chi)}{4} + C_J \delta(1-\chi)$$

$$T_{q\bar{q}G}(\chi) K_{q\bar{q}G}(\chi) = \frac{2\alpha_s}{\pi} \frac{1}{(1+\chi)(1-\chi)^5} \{4(5\chi^2+8\chi+5) \cdot \log((1+\chi)/2) + (\chi-1)(\chi^3-7\chi^2-16\chi-14)\} + C_K \delta(1-\chi), \quad (3.22)$$

where the coefficients of the delta functions are, as usual, infrared divergent constants. For $e^+e^- \to \zeta \to GGG$, one also finds

$$J_{GGG}(\chi) = -\tfrac{1}{4}, \quad (3.23)$$

while $K(\chi)$ for this case can be calculated using the results of [9]. The analytical results for $e^+e^- \to q\bar{q}G$ and $\zeta \to GGG$ are shown in Figs. 8 and 9 for both $J(\chi)$ and $K(\chi)$. The result $J(\chi) \equiv = \frac{1}{4}$ is a surprisingly common one [see (3.20)–(3.23)]. We know of no simple explanation for this (see Appendix A); it appears to be

Table 1. The beam moments $\langle \bar{\Xi}_k^l \rangle$ for $e^+e^- \to q\bar{q}$ at $\sqrt{s} = 20$ GeV[a]

	$l=0$: $\langle \bar{\Xi}_k^0 \rangle$	$l=3$: $\langle \bar{\Xi}_k^3 \rangle$	$l=0,2$: $\langle \bar{\Xi}_k^0 - \bar{\Xi}_k^2 \rangle$
$\langle \bar{\Xi}_0^l \rangle$, Hadrons	1	0.032	0.27
$\langle \bar{\Xi}_0^l \rangle$, FQGA	1	0	0
$\langle \bar{\Xi}_0^l \rangle$, Hadrons, $H_2/H_0 < 0.35$	0.001		
$\langle \bar{\Xi}_0^l \rangle$, FQGA, $H_2/H_0 < 0.35$	0		
$\langle \bar{\Xi}_1^l \rangle$, Hadrons	−0.047	−0.001	−0.013
$\langle \bar{\Xi}_1^l \rangle$, FQGA	−0.05	0	0
$\langle \bar{\Xi}_2^l \rangle$, Hadrons	0.0004	0.06	−0.001
$\langle \bar{\Xi}_2^l \rangle$, FQGA	0	0.1	0

[a] As usual, when not all the energy in the events is included in the calculation of the $\langle \bar{\Xi}_k^l \rangle$, the value in each event is divided by H_0 [1]. FQGA denotes the perturbative QCD calculation of the free quark and gluon final state

Table 2. The beam moments $\langle \bar{\Xi}_k^l \rangle$ for $e^+e^- \to q\bar{q}(G)$ at $\sqrt{s} = 20$ GeV[a]

	$l=0$: $\langle \bar{\Xi}_k^0 \rangle$	$l=3$: $\langle \bar{\Xi}_k^3 \rangle$	$l=0,2$: $\langle \bar{\Xi}_k^0 - \bar{\Xi}_k^2 \rangle$
$\langle \bar{\Xi}_0^l \rangle$, Hadrons	1	0.072	0.36
$\langle \bar{\Xi}_0^l \rangle$, FQGA	1	0.073	0.15
$\langle \bar{\Xi}_0^l \rangle$, Hadrons, $H_2/H_0 < 0.35$	0.09	0.018	0.067
$\langle \bar{\Xi}_0^l \rangle$, FQGA, $H_2/H_0 < 0.35$	0.028	0.015	0.02
$\langle \bar{\Xi}_1^l \rangle$, Hadrons	−0.044	−0.0027	−0.015
$\langle \bar{\Xi}_1^l \rangle$, FQGA	−0.048	−0.0027	−0.0076
$\langle \bar{\Xi}_1^l \rangle$, Hadrons, $H_2/H_0 < 0.35$	−0.0031	−0.0007	−0.0024
$\langle \bar{\Xi}_1^l \rangle$, FQGA, $H_2/H_0 < 0.35$	−0.0014	−0.0006	−0.0012
$\langle \bar{\Xi}_2^l \rangle$, Hadrons	0.0007	0.049	−0.002
$\langle \bar{\Xi}_2^l \rangle$, FQGA	0.0008	0.080	−0.0003
$\langle \bar{\Xi}_2^l \rangle$, Hadrons, $H_2/H_0 < 0.35$	0.00022	0.0011	−0.0002
$\langle \bar{\Xi}_2^l \rangle$, FQGA, $H_2/H_0 < 0.35$	0.00025	0.00040	0.00001

[a] As usual, when not all the energy in the events is included in the calculation of the $\langle \bar{\Xi}_k^l \rangle$, the value in each event is divided by H_0 [1]. FQGA denotes the perturbative QCD calculation of the free quark and gluon final state

Table 3. The beam moments $\langle \bar{\Xi}_k^l \rangle$ for $e^+e^- \to \zeta \to GGG$ at $\sqrt{s} = 10$ GeV[a]

	$l=0$: $\langle \bar{\Xi}_k^0 \rangle$	$l=3$: $\langle \bar{\Xi}_k^3 \rangle$	$l=0,2$: $\langle \bar{\Xi}_k^0 - \bar{\Xi}_k^0 \rangle$
$\langle \bar{\Xi}_0^l \rangle$, Hadrons	1	0.19	0.69
$\langle \bar{\Xi}_0^l \rangle$, FQGA	1	0.22	0.38
$\langle \bar{\Xi}_1^l \rangle$, Hadrons	−0.014	−0.0017	−0.0093
$\langle \bar{\Xi}_1^l \rangle$, FQGA	−0.04	0.0003	−0.019
$\langle \bar{\Xi}_2^l \rangle$, Hadrons	0.0008	0.0061	−0.0021
$\langle \bar{\Xi}_2^l \rangle$, FQGA	0.008	0.022	0

[a] As usual, when not all the energy in the events is included in the calculation of the $\langle \bar{\Xi}_k^l \rangle$, the value in each event is divided by H_0 [1]. FQGA denotes the perturbative QCD calculation of the free quark and gluon final state

"accidental". An isotropic (phase space) model would, of course, give zero for $J(\chi)$ and so the common nonzero value of $J(\chi)$ for the low order QCD processes in e^+e^- annihilation should provide a useful method of identifying them.

Inspection of (3.22) reverals that (ignoring delta function terms) both $J(\chi)$ and $K(\chi)$ tend to the values given in (3.20) for the pure $e^+e^- \to q\bar{q}$ process (with our prescription for defining the final plane) as $\chi \to \pm 1$. This supports our argument in the last section for the infrared stability of $\bar{\Xi}_k^l$; the equality of the $q\bar{q}$ and $q\bar{q}G$ values for $J(\chi)$ and $K(\chi)$ at $\chi = \pm 1$ will allow the infrared divergences to cancel between the contributions of the two final states. Remembering that the coefficient of $\delta(1-\chi)$ in $T(\chi)$ is just $C_T = 2\sum_i \langle E_i^2 \rangle / s$, we may form the infrared finite combinations of the coefficients of $\delta(1-\chi)$ in $J(\chi)$ and $K(\chi)$:

$$\begin{aligned} -\tfrac{2}{5}(C_J + C_T/4) &= \tfrac{4}{15}(C_K - 3C_T/8) \\ &= 2\left\langle \left(\sum_i E_i^2/s(P_2(\cos\alpha_i) - \tfrac{1}{10}) \right) \right\rangle \\ &= -2\alpha_s/15\pi, \end{aligned} \tag{3.24}$$

where α_i is the angle between particle i and the beam. The infrared finiteness of these combinations of $\delta(1-\chi)$ terms on their own occurs only at $0(\alpha_s)$. In higher orders, only the complete moments $\langle \bar{\Xi}_k^l \rangle$ integrated over all possible final state configurations will be infrared finite. It is amusing that the result $J(\chi) = -\frac{1}{4}$ for $e^+e^- \to q\bar{q}G$ is only violated in the coefficient of $\delta(1-\chi)$ to $0(\alpha_s)$.

3.5. *Some Results on $\tilde{F}_2^{pt}$ and its Moments $\bar{\Xi}_k^l$ for Hadronic Events*

The observables $J(\chi) = \langle P_2(\cos\theta_N) \rangle$ and $K(\chi) = \langle \sin^2\theta_N \cos(2\phi_N) \rangle$ introduced in Sect. 3.3 are shown in Figs. 8 and 9 as a function of χ for events of several types, both in the free quark and gluon approximation, and for simulated hadronic final states. $J(\chi)$ and $K(\chi)$ completely specify the dependence of $\tilde{F}_2^{pt}$ on the orientation of the two detectors with respect to the beam direction. The most striking feature of the curves in Figs. 8 and 9 is the similarity between results from the different QCD processes. An isotropic model with $J(\chi) = K(\chi) \equiv 0$ would be easy to distinguish from the QCD reactions. These figures also confirm that our simple model for $q\bar{q}$ fragmentation reproduces rather well the hadron final state angular functions given by the full Monte Carlo calculation. The effects of hadron fragmentation are minor except for the GGG final state and even there the hadron final states show beam correlations very different from the isotropic case.

In Tables 1 through 3, we give the mean values of the moments defined in Sect. 3.3. These are infrared stable and probably preferable to $J(\chi)$ and $K(\chi)$ discussed above. The latter have particular problems near $\chi=1$ which are properly averaged in the moments. The tables give $\langle\bar{\Xi}_k^0\rangle$, $\langle\bar{\Xi}_k^3\rangle$ and $\frac{3}{2}\langle\Xi_k^0\rangle=\langle\bar{\Xi}_k^0\rangle-\langle\bar{\Xi}_k^2\rangle$. $\bar{\Xi}_k^0$ is the simplest moment and provides the cleanest tests of the theory with the smallest effects from hadron fragmentation. In fact, the effects of hadron fragmentation appear to be less severe in $\bar{\Xi}_k^0$ than in the analogous single energy correlation in B_2 discussed in [1]. We currently consider $\bar{\Xi}_{1,2}^0$ as the best way of measuring beam angular dependence of the energy distribution of e^+e^- annihilation final states. $\langle\bar{\Xi}_k^3\rangle$ has a weighting function $P_3(\cos\chi)$ that is odd in χ and so is useful for investigating $K(\chi)$, which is predicted to be approximately odd in χ. Thus $\langle\bar{\Xi}_2^0\rangle$ and $\langle\Xi_2^0\rangle$ should always be small while $\langle\bar{\Xi}_2^3\rangle$ provides a measure of the absolute magnitude of K. We have not discussed the simplest odd function $\langle\bar{\Xi}_k^1\rangle$ because of its sensitivity to missing particles in incomplete final states observed experimentally (recall that $\langle\bar{\Xi}_0^1\rangle=\langle H_1\rangle$ vanishes because of momentum conservation). Finally the tables show $\frac{3}{2}\langle\Xi_k^0\rangle$, which is the simplest example of a moment observable with an explicit $\sin^2\phi$ suppression of the $\chi=\pm1$ regions.

Tables 1 and 2 also show results with an H_2 cut <0.35 (applied to the final hadrons) which selects "true" 3 jet events. The fact that these results are similar to those without the H_2 cut is an indication that the beam correlations do not depend importantly on the "shapes" of the events.

4. Three-Detector Energy Correlations

4.1. $F_{3\perp}$ as a Test for Planar Structure

In this section we consider the three-detector energy correlation, defined by

$$\tilde{F}_3(\sigma_1,\sigma_2,\sigma_3)=\frac{64\pi^3}{|\sigma_1|\,|\sigma_2|\,|\sigma_3|}\,\frac{|\mathbf{p}_1|\,|\mathbf{p}_2|\,|\mathbf{p}_3|}{(\sqrt{s})^3}, \tag{4.1}$$

where detector i has area $|\sigma_i|$ on which a total momentum $|\mathbf{p}_i|$ is incident. We shall consider only the function $F_3(\sigma_1,\sigma_2,\sigma_3)$ obtained by averaging over all positions of the detectors that maintain their relative orientation. Thus we ignore the correlations with the beam direction that were treated in Sect. 5 for the two detector case. The main purpose in considering three detector correlations is to find tests for planar momentum configurations. Two particle final states contribute to the two detector energy correlation function only when the angle between the two detectors is near 180°. On the other hand, three particle final states, as from $e^+e^-\to q\bar{q}G$ or $e^+e^-\to\zeta\to GGG$, have no such simple signatures in the two detector case. However, the momenta in the three particle final state lie in a plane and hence the three detector energy correlation vanishes for such events unless the detectors themselves are nearly coplanar. In order to extract the most demanding test of coplanarity, we define $F_{3\perp}$ as the value of the rotationally averaged $F_3(\sigma_1,\sigma_2,\sigma_3)$ when all the three detector directions are mutually orthogonal. We take the three detectors to be circular and of equal angular radius $\cos^{-1}(\delta)$. The normalization of F_3 is such that it has the value one for isotropic events. Thus the value of $F_{3\perp}$ is zero for idealized three jet events and one for isotropic events. Hence a measurement of $\langle F_{3\perp}\rangle$ provides a method for distinguishing these two event structures. Of course, the naive prediction that $\langle F_{3\perp}\rangle=0$ for three-jet events is only true at infinite energy, where there are neither perturbative nor hadronic corrections. At finite energies which are sufficiently large that fragmentation is unimportant, one may estimate that $\langle F_{3\perp}\rangle=(\alpha_s^2+0(\alpha_s^3)$ for $e^+e^-\to q\bar{q}(GG\ldots)$, while for $\zeta\to GGG(GG\ldots)$, $\langle F_{3\perp}\rangle\simeq\lambda'\alpha_s+0(\alpha_s^2)$. (Analogous results hold for $\langle\Pi_1\rangle$.) There are identications that λ and λ' are or order one [4]. Note that the decay $\zeta\to GGGG$ (which gives rise to non-coplanar final states) where ζ is, as above, a ${}^3S_1\,Q\bar{Q}$ state, is not forbidden by symmetry (as would the corresponding positronium decay) because the gluons can be antisymmetric in color. Hence, one expects that, at values of $\sqrt{s}$ for which fragmentation is unimportant, $\langle F_{3\perp}\rangle$ should be larger on resonances than in the continuum by a factor of order $1/\alpha_s$. For lower $\sqrt{s}$, the hadronization of the final state will modify perturbative predictions for $\langle F_{3\perp}\rangle$, and one must make a model to study the size of the changes. We consider the particular question of to what extent a measurement of $\langle F_{3\perp}\rangle$ enables one to test for 3 jet decay of the Υ and possible higher mass heavy quark bound states. In our calculations of the effects of fragmentation, we ignore the perturbative $0(\alpha_s)$ or $0(\alpha_s^2)$ corrections to the result $\langle F_{3\perp}\rangle=0$ for two and three jet events. We compare only mechanisms that lead to the same single hadron momentum distributions. We found [10] two models that gave the same z distributions as $e^+e^-\to\zeta\to GGG$. The first was obtained by construction; we generated hadrons from genuine $\zeta\to GGG$ events and then randomly rotated each hadron in the final state. We term this model "isotropic". For the second model, we noted that $e^+e^-\to M\bar{M}$, where each meason M decays into 3 jets (cf. Sect. 2.5), happens to give essentially the same single hadron momentum distribution as $e^+e^-\to\zeta\to GGG$. This "6 jet" model is, of course, not isotropic but it is certainly more so than would be

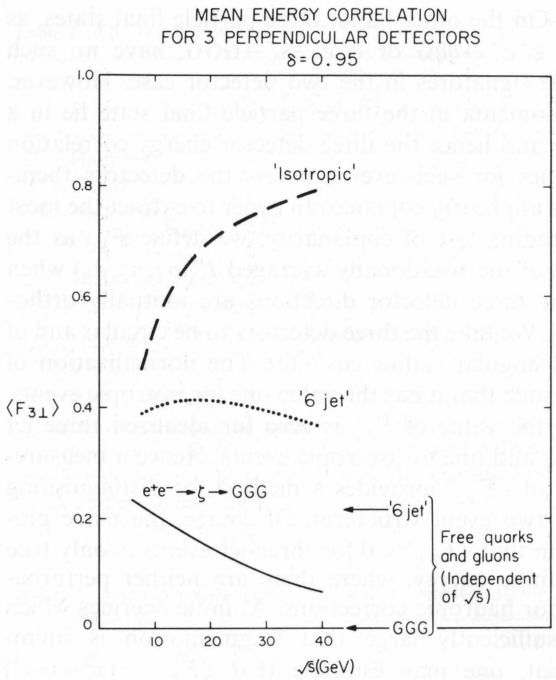

Fig. 10. The mean energy correlation $\langle F_{3\perp}\rangle$ between three orthogonal detectors with angular radii $\cos^{-1}(0.95)\simeq 18°$, as a function of $\sqrt{s}$, for three classes of processes discussed in the text. At infinite energy, coplanar events such as $\zeta\to GGG$ give $\langle F_{3\perp}\rangle=0$, while a completely isotropic distribution of energy in the final state gives $\langle F_{3\perp}\rangle=1$. "6 jet" final states give $\langle F_{3\perp}\rangle\simeq 0.2$ as $\sqrt{s}\to\infty$

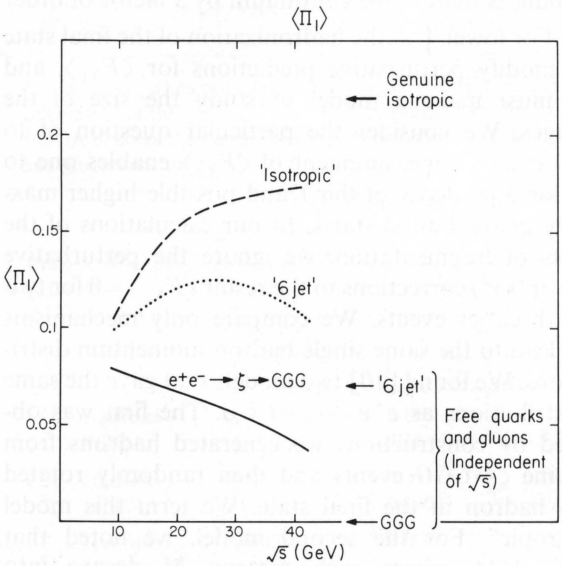

Fig. 11. The mean coplanarity parameter $\langle \Pi_1\rangle$ defined in Sect. 6.2 as a function of s. At infinite $\sqrt{s}$, $\zeta\to GGG$ gives $\langle \Pi_1\rangle=0$, isotropic events $\langle \Pi_1\rangle=2/9$ and "6 jet" ones $\langle \Pi_1\rangle\simeq 0.07$

expected from a GGG final state. In Fig. 10 we plot $\langle F_{3\perp}\rangle$ as a function of $\sqrt{s}$ for these three types of events. The GGG final state is easily distinguished, even at the Υ mass, from the more isotropic mechanisms. Of course, the discrimination improves as $\sqrt{s}$ increases.

Although $\langle F_{3\perp}\rangle$ appears to be a very useful experimental observable, we should point out that it is not trivial to calculate. We found no simple analogue of (2.1) for the two detector case. Thus we calculated $\langle F_{3\perp}\rangle$ by doing the angular average (integral) in its definition by a simple Monte Carlo technique. Note that this integral has to be done separately for each event.

We have chosen to emphasize one particular angular configuration for the three detectors: the case where they are mutually perpendicular. One can, of course, consider other angular separations but we do not believe they will lead to qualitatively different results.

4.2. *Moments of Three-Detector Energy Correlations*

The two jet form for the H_l:

$$\begin{aligned}\langle H_l\rangle&=0 \quad l \text{ odd}\\ \langle H_l\rangle&=1 \quad l \text{ even}\end{aligned} \tag{4.2}$$

is a moment analogue of the result for the two detector energy correlation:

$$F_2^{pt}(\chi)=\delta(1-\chi)+\delta(1+\chi)\,. \tag{4.3}$$

It is natural to ask if there is a moment analogue for the prediction that the three detector correlation function F_3^{pt} is zero for three particle final states unless the detectors are coplanar. In [10], we showed that there were such moment analogues but did not discuss their relation to F_3^{pt}. We defined two classes of moments that vanished for planar events:

$$\begin{aligned}\Pi_S&=\sum_{i,j,k}\frac{|\mathbf{p}_i|\,|\mathbf{p}_j|\,|\mathbf{p}_k|}{(\sqrt{s})^3}(\hat{p}_i\times\hat{p}_j\cdot\hat{p}_k)^2\,S(\hat{p}_i,\hat{p}_j,\hat{p}_k)\\ \Psi_A&=\sum_{i,j,k}\frac{|\mathbf{p}_i|\,|\mathbf{p}_j|\,|\mathbf{p}_k|}{(\sqrt{s})^3}(\hat{p}_i\times\hat{p}_j\cdot\hat{p}_k)\,A(\hat{p}_i,\hat{p}_j,\hat{p}_k)\,,\end{aligned} \tag{4.4}$$

where the functions S and A are respectively symmetric and antisymmetric polynomials in the scalar products of the unit vectors $\hat{p}_i$ in the directions of the particles i. The simplest example of the Π class of observables has $S=1$ and was denoted Π_1, while the simplest non-trivial member of the Ψ class (denoted by Ψ_1) has

$$\begin{aligned}A=[&(\hat{p}_i\cdot\hat{p}_k)^2(\hat{p}_k\cdot\hat{p}_j)+(\hat{p}_j\cdot\hat{p}_i)^2(\hat{p}_i\cdot\hat{p}_k)\\ &+(\hat{p}_k\cdot\hat{p}_j)^2(\hat{p}_j\cdot\hat{p}_i)-(\hat{p}_i\cdot\hat{p}_j)^2(\hat{p}_j\cdot\hat{p}_k)\\ &-(\hat{p}_k\cdot\hat{p}_i)^2(\hat{p}_i\cdot\hat{p}_j)-(\hat{p}_j\cdot\hat{p}_k)^2(\hat{p}_k\cdot\hat{p}_i)]\,.\end{aligned}$$

It is clear from our previous arguments that the moments of Π_S and Ψ_A are infrared stable when computed in QCD perturbation theory. As discussed in [10], we found Π_1 to be the most useful observable in that it offered the greater discrimination between 3 jet and isotropic processes at the Υ mass. In Fig. 11 we show $\langle \Pi_1 \rangle$ as a function of $\sqrt{s}$ for the three processes discussed in the previous subsection. There are again reasonably large differences between the results for $e^+e^- \to \zeta \to GGG$ events and for our models with isotropic ζ decay. However, comparison of Figs. 10 and 11 shows that $\langle F_{3\perp} \rangle$ is somewhat better than $\langle \Pi_1 \rangle$ at distinguishing the processes. Π_1 does have two advantages, however: first, it is much easier to calculate than $\langle F_{3\perp} \rangle$, and further it is not only possible to find easily the mean $\langle \Pi_1 \rangle$ but also the distribution $1/\sigma\, d\sigma/d\Pi_1$. The latter provides additional discrimination as discussed in [10].

We now describe the relationship of the observables Π_S and Ψ_A to F_3^{pt}; the analogue to the result that the H_l are the Legendre moments of F_2^{pt}. We specialize to the idealized case of point detectors and write F_3^{pt} in the rather formal manner

$$F_3^{pt}(\hat{\Omega}_{d1}, \hat{\Omega}_{d2}, \hat{\Omega}_{d3}) = 8\pi \int d\hat{\Omega}\, \varrho(\hat{\Omega}\hat{\Omega}_{d1})\varrho(\hat{\Omega}\hat{\Omega}_{d2})\varrho(\hat{\Omega}\hat{\Omega}_{d3}). \tag{4.5}$$

Here $\hat{\Omega}$ and $\hat{\Omega}_{dk}$ $(k=1,2,3)$ are elements of the rotation group. $\hat{\Omega}$ runs over all rotations (labeled by 3 Euler angles so that $\int d\hat{\Omega} = 8\pi^2$) while $\hat{\Omega}_{dk}$ is defined so that the direction of detector k is given by $\hat{\Omega}_{dk}\hat{z}$ where $\hat{z}$ is unit vector in the z direction. We have written (4.5) for the case of a continuous energy density ϱ normalized to unity when integrated over *independent* values of its argument (i.e., dropping the redundant azimuthal integral in $d\hat{\Omega}$), so that

$$\int d\hat{\Omega}\, \varrho(\hat{\Omega}) = 2\pi \tag{4.6}$$

and $\varrho = 1/4\pi$ for an isotropic event. Of course, for a particle event (4.5) is valid with ϱ as a sum of delta functions at the angles of the various particles. We now define the multipole moments A_l^m as in [1] and [10]:

$$A_l^m = \frac{1}{2\pi} \int d\hat{\Omega}\, \varrho(\hat{\Omega})\, Y_l^m(\hat{\Omega}) \tag{4.7}$$

or conversely

$$\varrho(\hat{\Omega}) = \sum_{l,m} A_l^m \sqrt{\frac{2l+1}{4\pi}}\, D_{m0}^l(\hat{\Omega}) \tag{4.8}$$

where $D_{mm'}^l$ are the conventional rotation matrices which can be written as

$$D_{m0}^l(\hat{\Omega}) = \exp(-\mathrm{i}m\phi)\, d_{m0}^l(\theta), \tag{4.9}$$

where

$$\hat{\Omega} = \hat{R}_z(\phi)\hat{R}_y(\theta)\hat{R}_z(\psi) \tag{4.10}$$

is expressed as a product of rotations about the y and z axes.

Substituting (4.8) into (4.5), we use the addition theorem for the D matrices to find

$$\begin{aligned} F_3^{pt}(\hat{\Omega}_{d1}, \hat{\Omega}_{d2}, \hat{\Omega}_{d3}) = & \sum_{\substack{l_1 l_2 l_3 \\ m_1 m_2 m_3 \\ m_1' m_2' m_3'}} \int d\hat{\Omega}\, D_{m_1 m_1'}^{l_1}(\hat{\Omega}) \\ & \cdot D_{m_2 m_2'}^{l_2}(\hat{\Omega}) D_{m_3 m_3'}^{l_3}(\hat{\Omega}) \\ & A_{l_1}^{m_1} A_{l_2}^{m_2} A_{l_3}^{m_3} D_{m_1 0}^{l_1}(\hat{\Omega}_{d1}) D_{m_2 0}^{l_2}(\hat{\Omega}_{d2}) \\ & \cdot D_{m_3 0}^{l_3}(\hat{\Omega}_{d3}) \sqrt{\frac{(2l_1+1)(2l_2+1)(2l_3+1)}{\pi}}. \end{aligned} \tag{4.11}$$

Defining the rotationally invariant three detector moments $T_{l_1 l_2 l_3}$ by

$$T_{l_1 l_2 l_3} = (4\pi)^{3/2} \sum_{m_1 m_2 m_3} \begin{pmatrix} l_1 l_2 l_3 \\ m_1 m_2 m_3 \end{pmatrix} A_{l_1}^{m_1} A_{l_2}^{m_2} A_{l_3}^{m_3} \tag{4.12}$$

the integral $d\hat{\Omega}$ may be expressed in terms of $3-j$ symbols [11] so that

$$F_3^{pt}(\hat{\Omega}_{d1}, \hat{\Omega}_{d2}, \hat{\Omega}_{d3}) = \sum_{l_1 l_2 l_3} T^{l_1 l_2 l_3} \Lambda^{l_1 l_2 l_3}(\hat{\Omega}_{d1}, \hat{\Omega}_{d2}, \hat{\Omega}_{d3}), \tag{4.13}$$

where

$$\begin{aligned} \Lambda^{l_1 l_2 l_3}(\hat{\Omega}_{d1}, \hat{\Omega}_{d2}, \hat{\Omega}_{d3}) = & \sqrt{(2l_1+1)(2l_2+1)(2l_3+1)} \\ & \sum_{m_1 m_2 m_3} \begin{pmatrix} l_1 l_2 l_3 \\ m_1 m_2 m_3 \end{pmatrix} D_{m_1 0}^{l_1}(\hat{\Omega}_{d1}) D_{m_2 0}^{l_2}(\hat{\Omega}_{d2}) D_{m_3 0}^{l_3}(\hat{\Omega}_{d3}). \end{aligned} \tag{4.14}$$

Λ is a function of general mathematical interest. It is a rotationally invariant function of three directions. This invariance can be expressed as

$$\Lambda^{l_1 l_2 l_3}(\hat{R}\hat{\Omega}_{d1}, \hat{R}\hat{\Omega}_{d2}, \hat{R}\hat{\Omega}_{d3}) = \Lambda^{l_1 l_2 l_3}(\hat{\Omega}_{d1}, \hat{\Omega}_{d2}, \hat{\Omega}_{d3}) \tag{4.15}$$

for any rotation $\hat{R}$. Λ is the three-direction analogue of the two-direction rotationally-invariant function $P_l(\hat{\Omega}_{d1}^{-1}\hat{\Omega}_{d2})$. Of course, the H_l are the two direction analogues of $T^{l_1 l_2 l_3}$ and F_2^{pt} can be expressed in terms of H_l and $P_l(\hat{\Omega}_{d1}^{-1}\hat{\Omega}_{d2})$ in analogy to (6.13). If any l value is zero, $\Lambda^{l_1 l_2 l_3}$ and $T^{l_1 l_2 l_3}$ reduce to $P_l(\hat{\Omega}_{d1}^{-1}\hat{\Omega}_{d2})$ and H_l, respectively.

Note that if $l_1 + l_2 + l_3$ is even, then T and Λ are real and invariant under any permutation of indices $\{k\}$ in the l_k and $\hat{\Omega}_{dk}$. On the other hand, if $l_1 + l_2 + l_3$ is odd, then both T and Λ are purely imaginary and permutations of $\{k\}$ multiply them by the signature of the permutation.

This fact leads to our first test for planes. If in a planar event we choose the x and z axes to be in the

plane, then the A_l^m are manifestly purely real and hance all $T^{l_1 l_2 l_3}$ are real. Therefore, $T^{l_1 l_2 l_3}$ vanishes for planar events if $l_1+l_2+l_2$ is odd. The simplest nontrivial constraint corresponds to $T^{234}=0$ and one can easily show that

$$\Psi_1=\tfrac{8}{35}\mathrm{Im}(T^{234}). \tag{4.16}$$

The equivalence between Ψ-like tests [in sense of (4.4)] and $\mathrm{Im}(T^{l_1 l_2 l_3}; l_1+l_2+l_3$ odd) is complete. Note that both Ψ_A and $\mathrm{Im}(T^{l_1 l_2 l_3})$ are pseudoscalars (i.e., change sign on reversal of all the particle momenta) while Π_S and $\mathrm{Re}(T^{l_1 l_2 l_3})$ are scalars.

We now show how to obtain observables of the Π type from our new formalism. We first choose a particular configuration for the three detectors with detector 1 along the z axis and detector 2 in the xz plane:

$$\begin{aligned}\hat{\Omega}_{d1}&=1\\ \hat{\Omega}_{d2}&=\hat{R}_y(\theta_2)\\ \hat{\Omega}_{d3}&=\hat{R}_z(\phi_3)\hat{R}_y(\theta_3).\end{aligned} \tag{4.17}$$

This makes the degrees of freedom of Λ manifest but loses the elegant symmetry of the original form (4.14). We can now express F_3^{pt} as a Fourier series in the azimuthal variable ϕ_3:

$$\begin{aligned}F_3^{pt}(\theta_2,\theta_3,\phi_3)&=\sum_m \Gamma^m(\theta_2,\theta_3)\exp(\mathrm{im}\,\phi_3)\\ &=2\sum_{m\geqq 0}(\mathrm{Re}\,\Gamma^m)\cos m\phi_3\\ &\quad-2\sum_{m>0}(\mathrm{Im}\,\Gamma^m)\sin m\phi_3,\end{aligned} \tag{4.18}$$

where

$$\Gamma^m(\theta_2,\theta_3)=\sum_{l_1 l_2 l_3}\sqrt{(2l_1+1)(2l_2+1)(2l_3+1)}\;T^{l_1 l_2 l_3}\begin{pmatrix} l_1 & l_2 & l_3\\ 0 & m & -m\end{pmatrix} d^{l_2}_{m0}(\theta_2)d^{l_3}_{-m0}(\theta_3). \tag{4.19}$$

For a planar event, F_3^{pt} is proportional to a delta function at $\phi_3=0$, and inverting the Fourier series (4.18) this implies

$$\mathrm{Im}\,\Gamma^m=0 \qquad (m \text{ integer}), \tag{4.20}$$

$$\mathrm{Re}\,\Gamma^m=\mathrm{Re}\,\Gamma^{m'} \qquad (m,m' \text{ integer}). \tag{4.21}$$

The result (4.20) is just vanishing of $\mathrm{Im}(T^{l_1 l_2 l_3})$ for planar events that we have already discussed. Some of the information in (4.21) can be turned into new moment constraints that are equivalent to $\Pi_S=0$ in (6.4). Consider the relation

$$\mathrm{Re}\,\Gamma^{m_1}=\mathrm{Re}\,\Gamma^{m_2} \quad m_1>m_2, \tag{4.22}$$

where m_1 and m_2 differ by an even integer. Multiply both sides of (4.22) by $d^{l_2}_{m_1 0}(\theta_2)d^{l_3}_{-m_1 0}(\theta_3)$ and integrate $d(\cos\theta_2)d(\cos\theta_3)$. Using the orthogonality of the d matrices, we pick up a finite linear combination of $T^{l_1 l_2 l_3}$ (l_2, l_3 fixed, l_1 varies) on the left hand side. Now we can express $d^{l_2}_{m_1 0}(\theta_2)$ as a linear combination of $d^{l'_2}_{m_2 0}(\theta_2)$ with $l'_2\leqq l_2$ and similarly for l_3. (Here we use our choice that m_1 and m_2 differ by an even integer.) It follows that the right hand side is also a finite linear combination of $T^{l_1 l_2 l_3}$ observables and hence (4.22) gives rise to a set of finite relations between $\mathrm{Re}\,T^{l_1 l_2 l_3}$ for planar events. These relations may be translated into constraints of the form $\Pi_S=0$. For example, the simplest observable Π_1 is obtained from the relation $\mathrm{Re}\,\Gamma^2=\mathrm{Re}\,\Gamma^0$ on multiplying through by $d^2_{20}(\theta_2)d^2_{-20}(\theta_3)$ and integrating. Reference [10] gives some of the simpler Π observables found in this way as linear combinations of the $T^{l_1 l_2 l_3}$.

Appendix A: $2+\sin^2\theta_N$ Forever?

A remarkable feature of the results presented in Sect. 4.2 was that four distinct processes gave a $2+\sin^2\theta_N$ distribution for the angle θ_N between the incoming beam direction and the normal to the plane defined by the (three-particle) final state: $e^+e^-\to q\bar{q}G$, $e^+e^-\to\zeta(^3S_1)\to GGG$, $e^+e^-\to q\bar{q}\phi$, where ϕ is a scalar "gluon" and $e^+e^-\to q\bar{q}$, where the plane in this case is taken to have a uniform distribution about the $q\bar{q}$ direction. One may wonder whether this common $2+\sin^2\theta_N$ dependence is accidental or has some fundamental significance. As we will now describe, our tentative conclusion is that it is largely accidental.

The formalism of Sect. 3.2 shows that a $2+\sin^2\theta_N$ distribution has a simple interpretation in terms of the amplitudes E_λ for virtual photons of helicity λ to decay to a given final state configuration. We work in the virtual photon rest frame and quantize the photon spin along the normal to the plane defined by the final state particles. Then the condition for a $2+\sin^2\theta_N$ angular distribution is

$$|E_0|^2=|E_1|^2+|E_{-1}|^2. \tag{A.1}$$

This may also be expressed as a constraint on the photon polarization amplitude A_μ. If z is the normal to the final state plane, and the x and y are axes in the plane, then (A.1) may be rewritten as

$$|A_z|^2=|A_x|^2+|A_y|^2. \tag{A.2}$$

Note that gauge invariance for a photon at rest implies

$$|A_0|^2=0. \tag{A.3}$$

We first discuss the origin of the $2+\sin^2\theta_N$ behavior in the process $e^+e^-\to q\bar{q}G$. As mentioned in Sect. 3.4, this angular distribution is easy to understand in the infrared limit where the virtual quark is nearly on shell. Here, the gluon will be distributed uniformly in azimuth about the $q\bar{q}$ direction, while the q and $\bar{q}$ will have a $1+\cos^2\theta$ angular distribution with respect to the beam direction. In this limit, therefore, $e^+e^-\to q\bar{q}G$ behaves like $e^+e^-\to q\bar{q}$ with random plane orientation, and the $2+\sin^2\theta_N$ form follows directly. The same result holds for scalar gluons. Unfortunately, these arguments cannot be extended away from the infrared region where the q and $\bar{q}$ no longer have a $1+\cos^2\theta$ angular distribution. In Feynman gauge, one finds that for each of the two diagrams contributing to $e^+e^-\to q\bar{q}G$,

$$|A_z|^2=|A_x|^2+|A_y|^2-|A_0|^2. \tag{A.4}$$

However, only in the sum of the diagrams does the $|A_0|^2$ term cancel so that the requirement (A.2) is satisfied. The fact that all diagrams must be included (at least in Feynman gauge) in order to obtain a $2+\sin^2\theta_N$ angular distribution for $e^+e^-\to q\bar{q}(G)$ suggests that its appearance there is somewhat "accidental".

For $e^+e^-\to\zeta\to GGG$, the situation is even more mysterious. In this case, two heavy quarks annihilate at rest leaving no hint of a $1+\cos^2\theta$ beam distribution which might be transmuted into a $2+\sin^2\theta_N$ plane angular distribution. In fact, one can easily show that the $2+\sin^2\theta_N$ obtained for ζ decay to spin 1 gluons does not hold for spin 0 gluons. For scalar gluons, $E_0=0$, while for pseudoscalar ones, $E_1=E_{-1}=0$.

We conclude that we are unable to find a fundamental explanation for the widespread $2+\sin^2\theta_N$ behavior. Perhaps the reader can.

Appendix B: "Scalar QCD"

In assessing to what extent various measurements constitute tests of QCD, it is convenient to compare QCD predictions for them with results obtained from other theories. In this appendix, we give the forms for some of the results discussed in this paper which would follow from a theory in which the gluons (ϕ) are colored scalars (see also [12]). This theory has many fundamental differences from QCD. In particular, the effective $qq\phi$ coupling λ does not tend logarithmically to zero as s increases but rather goes to a constant value as a power of s. Nevertheless, this behavior is not yet ruled out by deep inelastic scattering measurements. The $\gamma^*\to q\bar{q}\phi$ differential cross-section is

$$\frac{d\sigma}{dx_1\,dx_2}=\frac{\lambda}{3\pi}\,\frac{x_3^2}{(1-x_1)(1-x_2)}. \tag{B.1}$$

Note that this exhibits collinear but not combined collinear and soft infrared divergences. Adding in the one-loop corrections to $\gamma^*\to q\bar{q}$, one finds that for scalar QCD, the e^+e^- total cross-section is[11]

$$\sigma=\sigma_0\left(1+\frac{\lambda}{2\pi}+\ldots\right). \tag{B.2}$$

From (B.1) one finds that for $e^+e^-\to q\bar{q}(\phi)$:

$$\langle H_2\rangle=1-\frac{\lambda}{3\pi}(21-2\pi^2)\simeq 1-0.13\lambda, \tag{B.3}$$

$$\langle H_3\rangle=\frac{20\lambda}{9}(7\pi^2-69)\simeq 0.19\lambda, \tag{B.4}$$

while for $e^+e^-\to q\bar{q}(G)$ [1]:

$$\langle H_2\rangle=1-\frac{2\alpha_s}{3\pi}(4\pi^2-33)\simeq 1-1.4\alpha_s, \tag{B.5}$$

$$\langle H_3\rangle=\frac{2\alpha_s}{9\pi}(1980-200\pi^2)\simeq 0.43\alpha_s. \tag{B.6}$$

For $e^+e^-\to q\bar{q}\phi$:

$$\begin{aligned}\langle F_2^{pt}(\chi)\rangle=\frac{2\lambda}{3\pi}\,\frac{1}{(\chi-1)^5(1+\chi)}\Big[&8(1+\chi)(2\chi^2+18\chi\\&+19)\log\left(\frac{1+\chi}{2}\right)\\&+(1-\chi)(47\chi^2+160\chi+105)\Big]+C\delta(1-\chi)\,,\end{aligned} \tag{B.7}$$

$$\langle F_2^{pt}(0)\rangle=\frac{2\lambda}{3\pi}(152\log 2-105)\simeq 0.076\lambda. \tag{B.8}$$

The corresponding results for $e^+e^-\to q\bar{q}G$ are given in Sect. 2.2. Equations (B.3) through (B.8) indicate that, for a given value of the coupling constant, scalar QCD predicts that continuum e^+e^- annihilation events should be closer to the two-jet limit than is expected from QCD.

11 For colored scalar quarks, but vector gluons, this result becomes

$$\sigma=\sigma_0\left(1+\frac{4\lambda}{\pi}+\ldots\right)$$

Near $\chi = -1$, the $\langle F_2^{pt}(\chi)\rangle$ given in (B.7) becomes

$$\frac{\lambda}{3\pi}\left[\frac{1}{(1+\chi)} + \frac{6\log\left(\frac{1+\chi}{2}\right) - 25}{4} + \ldots\right], \tag{B.9}$$

while around $\chi = +1$, the regular part goes like

$$\frac{\lambda}{3\pi}\left[\frac{1}{12(1-\chi)} + \frac{7}{30} + \ldots\right]. \tag{B.10}$$

Note the absence of a double logarithmic divergence in the integral of $\langle F_2^{pt}(\chi)\rangle$ close to $\chi = -1$. This implies [2] that the $\langle H_l\rangle$ for $e^+e^- \to q\bar{q}(\phi)$ depend on $\log(l)$ for large l, rather than $\log^2(l)$, as in QCD. The $\langle H_l\rangle$ at large l for the process $e^+e^- \to q\bar{q}(\phi\phi\ldots)$ behave like $l^{-a\lambda}$ when summed to all orders in λ, in contrast to the result $\sim l^{-b\alpha_s \log l}$ found in QCD.

Acknowledgements. We are grateful to the MATHLAB group of the MIT Laboratory for Computer Science for the use of MACSYMA.

References

1. G.C. Fox, S. Wolfram: Phys. Rev. Lett. **41**, 1581 (1978); Nucl. Phys. B**149**, 413 (1979)
2. G.C. Fox, S. Wolfram: Caltech preprint CALT-68-723 (August 1979)
3. C.L. Basham, L.S. Brown, S.D. Ellis, S.T. Love: Phys. Rev. D**17**, 2298 (1978); Phys. Rev. **41**, 1585 (1978); Phys. Rev. D**19**, 2018 (1979)
4. S. Wolfram: Caltech preprint CALT-68-740 (September 1979)
5. G.C. Fox, S. Wolfram: Caltech preprint CALT-68-755 (December 1979)
6. R.D. Field, R.P. Feynman: Nucl. Phys. B**136**, 1 (1978)
7. See, for instance, the results presented by JADE, MARK J, PLUTO and TASSO collaborations at the International Symposium on Lepton and Photon Interactions at High Energies, Fermilab, 1979
8. S.-Y. Pi, R.L. Jaffe, F.E. Low: Phys. Rev. Lett. **41**, 142 (1978)
9. K. Koller, T.F. Walsh: Nucl. Phys. B**140**, 449 (1978)
   K. Koller, H. Krasemann, T.F. Walsh: DESY 78/37, preprint (1978)
10. G.C. Fox, S. Wolfram: Phys. Lett. B**82**, 134 (1979)
11. M.E. Rose: Elementary theory of angular momentum. New York: Wiley 1957
12. C.L. Basham, S.T. Love: Phys. Rev. D**20**, 340 (1979)